Chapter 11

Production of Anti-Corrosion Coatings on Light Alloys (Al, Mg, Ti) by Plasma-Electrolytic Oxidation (PEO)

Riyad O. Hussein and Derek O. Northwood

Additional information is available at the end of the chapter

http://dx.doi.org/10.5772/57171

1. Introduction

As the world becomes increasingly more environmentally conscious, many countries are looking for ways to make products that are both safe for the environment and reduce or eliminate any health concerns for their workers. Considerable collaborative work has been done in the academic, industrial and governmental sectors to find environmentally compliant substitutes for chromium, particularly hexavalent chromium [1]. Sol-gel coatings and conducting polymers are being developed as either barrier coatings or reactive inhibitor systems to replace chromates for corrosion protection [2]. Conversion layers provide the ability to modify the substrate surface to give better adhesion, a surface free of contaminants or a coating layer that contains active corrosion inhibitors.

Among the newer surface modification techniques, plasma electrolytic oxidation (PEO) has recently been successfully applied to light-metals. The term 'light-metals' has traditionally been given to magnesium, aluminum and titanium because they are frequently used to reduce the weight of products due to their relative low densities. The plasma-assisted electrochemical surface treatment PEO process is capable of producing very thick coatings on the substrate materials to enhance their hardness, thermal resistance, dielectric strength, friction coefficient, and wear and corrosion resistance during relatively short time, in addition to its excellent throwing power (the ability of the process to deposit metal uniformly on an irregularly shaped cathode [3].

For PEO coating growth there are two simultaneous processes occurring, namely the electrochemical and the plasma chemical reactions. The plasma chemistry of the surface discharges is quite complex in nature, involving, on one hand, charge transfer at the substrate/electrolyte interface, and on the other hand, strong ionization and charge transfer effects between the substrate surface and the electrolyte through the oxide layer with the aid of the plasma [4].

The microstructure and phase content of the coatings are related to the process parameters and to their ultimate corrosion resistance. In this chapter a detailed description of the PEO-coating mechanism will be given supported by detailed diagrams and figures. The effects of the process parameters on the microstructure and associated corrosion resistance of the PEO coatings on Al, Ti and Mg alloys will also be discussed.

2. Surface modification and treatment for lightweight metals

So far, a number of theoretical and experimental studies had been performed addressing different aspects of the corrosion protection of lightweight metals and their alloys. Surface treatment/modification and coating occurs only on/or close to the surface layer of lightweight alloys and the bulk alloy is left unchanged hence the original mechanical or other properties are not changed.

An overview of the different techniques used for treatment or modification of Mg, Al and Ti alloys is shown in Fig.1 [2,5-6] and a comparison of the common surface treatments and coatings is given in Table 1. Generally, coatings can be divided into three classes: conversion coatings, organic and inorganic deposited coatings. Conversion coatings are produced by chemical or electrochemical reactions between the substrate and the aqueous solutions to form an oxide layer that simultaneously grows inwards and outwards. Such conversion coatings represent an effective way to increase the corrosion resistance of aluminum, magnesium and titanium alloys or, as a pre-treatment, to enhance the adhesion of a final deposited coating [2].

Treatment/coating	Drawback (general)	Drawback (environment)
Conversion (chromate, phosphate)	Easily damaged	Toxic, particularly Cr(VI)
Anodizing	Sensitive to impurities in the base metal to be coated	Sulphuric acid baths
Organic/polymer	Weak mechanical and corrosion resistant properties	Poor recyclability
Gas phase deposition (PVD, CVD)	Thin, porous	Chlorine emission
Thermal spray, cold spray	Not suitable for components with complex geometry. Use of more noble materials that can cause corrosion at interface	None
Plasma electrolytic oxidation	Lack of data on coating performance in practice	None

Table 1. A comparison of the common surface treatments and coatings for light-weight alloys. Adapted from [10]

http://dx.doi.org/10.5772/57171

Cost effective organic coating techniques, including sol-gel, painting and powder coating, are typically used after a primary surface-treatment of the substrate. The method most applied to obtain organic coatings is simple dipping in an organic based solution including: gelatin/PLGA particle solution, prospolis and polylactic-co-glycolic acid (PLGA) solution [7,8]. Metallic protective coatings can be produced from inorganic deposition coatings such as from the gas phase or other physical methods including plasma spraying, chemical vapor deposition (CVD), diamond like coatings (DLC) and lasers.

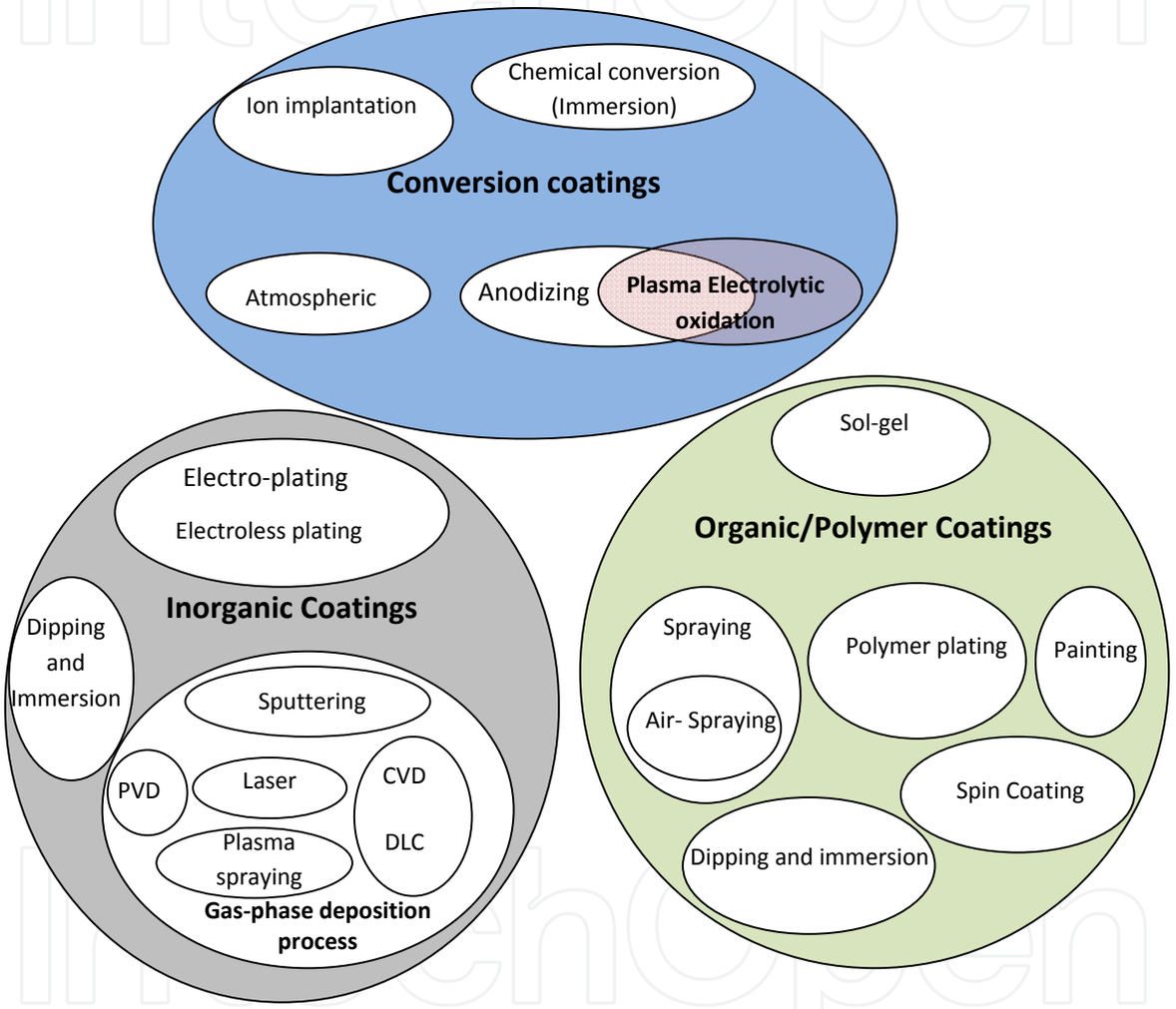

Figure 1. Schematic Diagram showing coating technologies [adapted from [5]].

Gas phase coatings are inappropriate for applications involving geometrically complex components. Moreover, physical deposition methods involve high energy consumption, high costs and complex facilities. The most common conversion layers are from electrochemical anodization. Recently, much research has been focused on the selection of electrolytes, including alkaline solutions with additives of phosphate, silicate, and borate substances. However, the anodizing process sometimes suffers from relatively poor performance. For example, the European Space Agency was having problems with the black anodizing process

[9]. A comparison between PEO and the hard anodization processes is given in Table 2. The PEO process can be considered as a combination of anodizing (electrolytic oxidation) and plasma discharging processes. Where, the main similarities between the PEO and anodizing processes, is that both of them involve oxidation of substrate using electrolytic bath and first stage of the PEO process is an anodization process. It is also common to combine two or more techniques for surface coating and/or modification, to obtain properties that are unattainable using an individual technique.

Process	PEO	HA
Voltage and current density	High	Low
Deposition rate	Fast (1~2μm/min)	Slow (~0.3μm/min)
Oxidation mechanism	Chemical/ electrochemical and plasma chemical reactions	Chemical/electrochemical reactions
Coating on selected alloys	Practical for various kinds of Al, Mg and Ti alloys	Limited (not used for 2000-series alloys, high zinc or silicon Al alloys and Al casting alloys)
Microstructure	Amorphous and crystalline phase / Inner dense layer and outer porous layer	Amorphous / Columnar porous layer and very thin barrier
Corrosion resistance (Relative)	Excellent (5)	Good (1)
Hardness	High (~Hv1600)	Low (Hv600 max)
Wear resistance (relative)	Excellent (30)	Fair (2)
Thermal protection	Excellent	Good
Electrolyte	Alkaline solution	Acid solution
Dielectric strength	Excellent	Fair

Table 2. Comparison of PEO with HA processes.

3. The PEO process: General comments

The formation of oxide films on metals were first investigated at the beginning of the twentieth century by Günterschulze and then Günterschulze and Betz [11]. They published their first studies on the electrolytic spark discharge produced on aluminum foil in the early 1930s. In the former Soviet Union in the 1960s and 70s, scientists investigated the anodizing process at potentials of over 200 volts for developing parts for the submarine sector and for military purposes. This led to plasma electrolytic oxidation (PEO) technology, which is also known as micro-arc oxidation (MAO) and micro-plasma oxidation (MPO). Hussein et al [12] have provided a detailed historical background of the process. It wasn't until the 1990s that the PEO process gained worldwide recognition as an eco-friendly technology for depositing the tribologically superior and excellent corrosion protection ceramic coatings on aluminum, titanium and magnesium alloys [12]. To date, thousands of a scientific publications dealing with a plasma electrolytic oxidation technology can be found in a wide variety of journals and conference proceedings.

http://dx.doi.org/10.5772/57171

Plasma Electrolyte Oxidation (PEO) is a novel surface engineering technology, considered as one of the most cost-effective and environmentally friendly ways to improve the corrosion and wear resistance of lightweight metals and their alloys [3]. A driving force for PEO developments is the avoidance of expensive equipment required for competing vacuum-based plasma technologies. The substrate is immersed in an aqueous electrolyte (containing neither the concentrated sulphuric acid nor the chromate ions used for hard anodizing) and a high anodic potential is applied to it (typically several hundreds of volts) that trigger numerous micro-discharge events at the metal-electrolyte interface, generating high instantaneous temperatures and pressures ($T > 40000$ K [4]) and $p \sim 100$ GPa, [3]). Different current modes have been utilized in the PEO treatment including, DC, AC, unipolar and bipolar current modes [13] which play important roles in the consequent voltage breakdown, local melting and oxidation of the substrate, quenching and re-crystallization processes. Hence, the formation mechanisms for the coatings are complex due to the involvement of electro-, thermal-, and plasma- chemical reactions in the electrolyte [12,14].

A schematic diagram of a commercial setup for PEO coating is shown in Figure 2 [12]. It consists of a stainless steel bath which contains the electrolyte, and which is often water-cooled, a high power electrical source and a pulse generator. The sample under treatment is connected to the output of the electrical source as one of the electrodes (anode), while being immersed in the bath of electrolyte solution. The stainless steel bath acts as a counter-electrode. The technology can be applied to coat a variety of materials, such as aluminum, magnesium, titanium, and zirconium. It can also be applied to alloys that are difficult to anodize with conventional anodizing processes, such as high copper content and high silicon content aluminum alloys (2000 series and A380), and magnesium alloys, with the deposition of layers such as phosphates, silicates and aluminates oxides. This enables the surfaces of metals such as titanium to be converted into very hard materials like TiN_2 or TiB_2. A key to the development of such coatings lies in the understanding and characterisation of the plasma processes involved in the individual discharges.

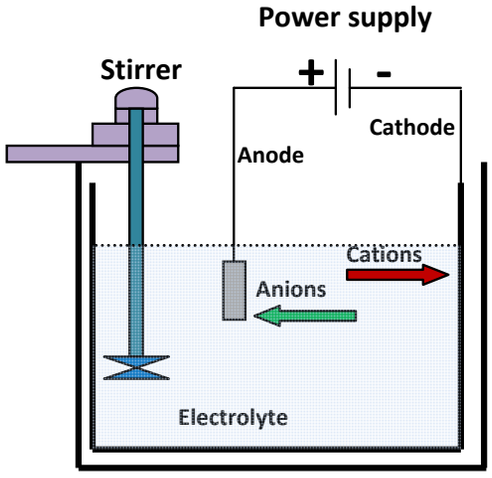

Figure 2. Schematic diagram of the PEO apparatus.

The PEO process can be distinguished from low voltage anodizing in aqueous solutions by its operation at electrode potentials greater than the typical breakdown voltages of the original oxide films (350-600 V) in AC, DC or pulsed AC/DC modes with asymmetric anodic and cathodic potential peak waveforms, depending on the alloy and electrolyte composition [4,12]. PEO also operates differently from high energy plasma coating under dry conditions in a controlled gas pressure chamber. It has been shown that PEO room temperature technology has a number of unique advantages: including technological simplicity and the possibility to coat any size and/or complex structure including welded and riveted joints, and heterogeneous alloys [15]. Pretreatments and post treatments are not strictly necessary for the PEO, except for water rinses; this reduces environmental concerns with respect to pretreatment and post treatment solutions. The PEO process is capable of producing uniform and very thick coatings on the inner and outer surfaces of the substrate materials [16]. One of the main advantages of the PEO coating is that the oxide coating is integral with the metal substrate because the coating is a result of substrate oxidation.

Fig. 3 show a typical Voltage vs. treatment time plots during the PEO processing of (a) AM50 Mg-alloy using a DC current mode and (b) an output anodic (V_A) and cathodic ($-V_C$) voltage vs time curves of an AJ62 Mg-alloy (MgAl6Mn0.3Sr2) using a bipolar current mode. Four consecutive discharge stages can be distinguished, namely: **Stage I:** In the early stage of the process which mainly involves the rapid electrochemical formation of an initial insulating oxide film, a sharp increase in the voltage was seen. In this stage the breakdown voltage is not yet reached. **Stage II:** The rate of the voltage change decreases in this stage, which is characterized by numerous sparks moving rapidly over the whole sample surface area. This indicates a start of the breakdown of the oxide layer, an increase in temperature and, therefore, melting of the substrate metal. **Stage III:** In this stage the rate of voltage increase becomes slow; this stage is characterized by larger but slower moving discharges. As the oxide layer grows, its electrical resistance increases, therefore the nature of the plasma changes. **Stage IV:** In this stage the rate of voltage variation is even slower than that in stage III and concentrated

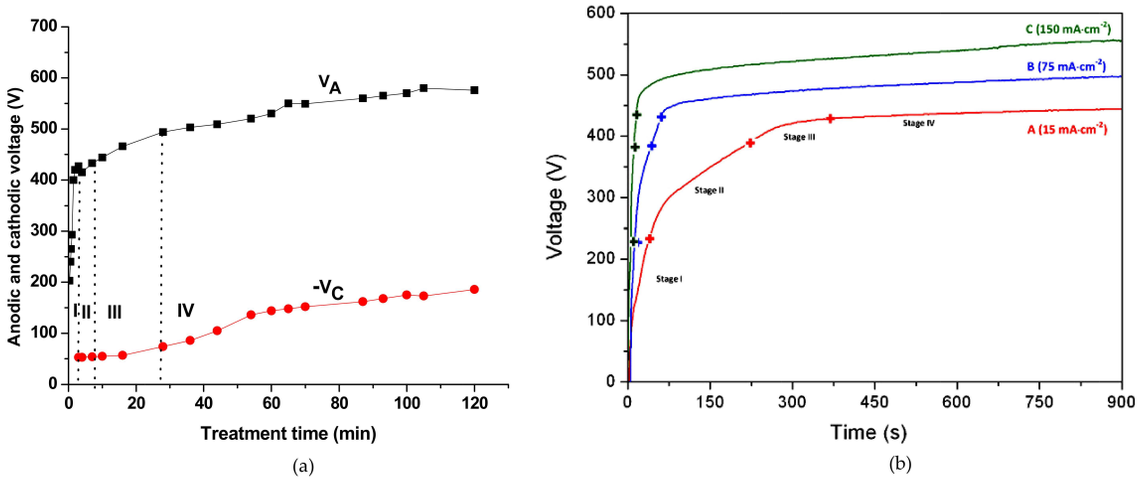

Figure 3. Voltage vs. treatment time during PEO processing of (a) AM50 Mg-alloy using DC current mode [18], (b) AJ62 Mg-alloy using a bipolar current mode showing anodic (V_A) and cathodic ($-V_C$) voltage parts [19].

http://dx.doi.org/10.5772/57171

discharges appear as relatively large and long lasting sparks. For some cases, such strong discharges may cause irreversible damage to the coatings in stage IV. Figure 4 shows a fast video imaging of the PEO coating showing the size and color of the micro discharges changing with time of an Al-alloy [17]. At the early stage of the process, intense gas evolution along with some luminescence at the surface is easily observed; this is followed by sparks flashing randomly all over the aluminum alloy surface, Figure 4(a), while sparks progressively change to micro-arcs (Figure 4(c)). Finally arcs regime, Figure 4(d,e) occurring at later stages of the process causing irreversible damages to the oxide layer.

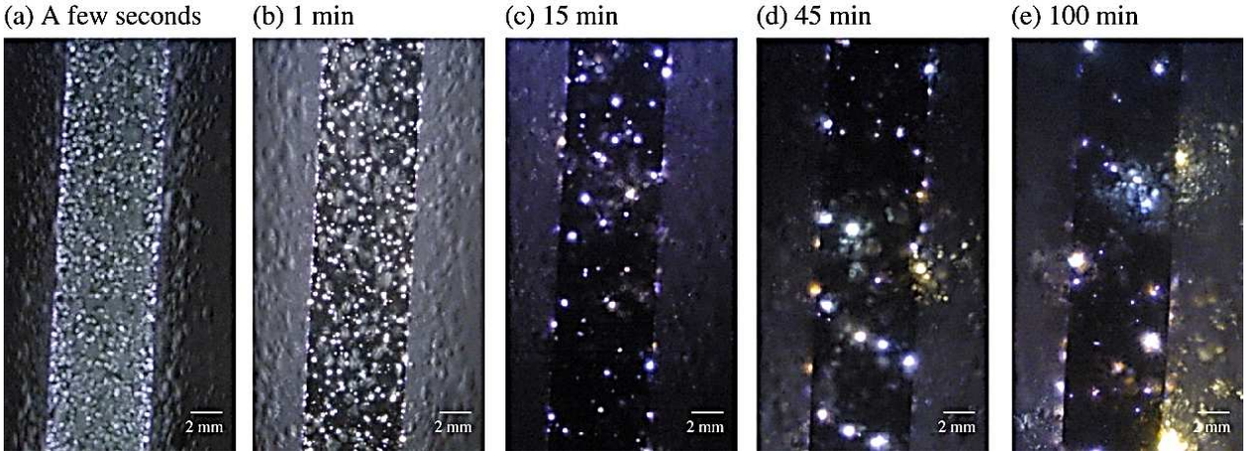

Figure 4. Fast video imaging of the PEO coating showing the size of the micro discharges changing with time [17].

4. PEO applications

Oxide coatings have been deposited on aluminum or magnesium alloys for the purposes of protection against wear and/or corrosion. Coatings on titanium have been investigated for potential applications relying on the biocompatibility or photo-activity of titania (TiO_2). Among the light alloys, Mg alloys are the most reactive and thus susceptible to corrosion, followed by Al alloys and Ti alloys. In general, such alloys need a specific coating thus allowing for a large range of possible applications across all industrial sectors

Depending on where they are used, the coatings should have resistance to chemicals, heat and electricity. PEO-coated products are used in a wide range of applications and industries see Figure 5, including:

i. **Decorative purposes or optical applications:** Depending on electrolyte composition and concentration, PEO processing parameters such as color additives and electrical parameters and chemical composition of substrate, the color of PEO coatings can be black, blue, gray, and white. By designing in porosity, a PEO pre-treatment can enhance the adhesion of paints, sol-gel and powder coatings and produce duplex coatings for enhanced properties particularly in aggressive media [9].

ii. **Thermal Applications:** The thermal conductivity of the PEO oxide layer is low and thermal cycling tests, have shown excellent performance at temperatures between -40 to +100°C. Thus, PEO coatings can be used to increase the thermal shock resistance [20].

iii. **Mechanical Applications (hardness, wear and friction):** Due to the high hardness and superior tribological performance of the oxide layer formed by PEO process, which for example reduces the wear rate of 6061 Al alloy by a factor of about 30 [21] compared to 2 times for the hard anodized coating, allows a replacement of many parts by PEO coated Mg and Al alloys leading to a reduction in fuel consumption in the automotive and aerospace industries. Improved coating performance that can be obtained has yielded applications for PEO technology in the aerospace industry (fasteners, landing gear, blades, discs and shafts of aircraft engines), the automotive industry (seat frames, doors, pistons and cylinder liners), and the gas and oil industries (gears and rotary pumps) [22].

Figure 5. Use of PEO coatings on: (a) engine piston, (b) racing yachts, (c) engine block and (d) dental implants.

i. **Electric and Electronic Applications:** Electrical insulation coatings can be obtained with high dielectric strength for electrical and electronic components. Also PEO is suitable for the hard coating of the inner areas including conic, cavital or cylindrical areas.

ii. **Chemical Applications:** PEO coatings can be used in chemical industries due to the coatings resistance to aqueous environments and resistance to strong acids and strong bases.

iii. **Biomedical applications:** Surface engineered titanium and magnesium alloys for biomedical devices including degradable biomaterials and dental implants [23].

5. Coating surface morphology and microstructure

The surface morphology and coating microstructure will have a significant impact on the corrosion behaviour which is governed by the level of porosity and defects as well as the thickness of the dense layer. Most of the studies discussed in this section used scanning electron microscopy (SEM) and transmission electron microscopy (TEM) to observe the surface and cross sections of the coatings.

http://dx.doi.org/10.5772/57171

The surface of PEO coatings typically show a 'pancake' structure wherein the center of each pancake was a discharge channel through which the molten elements surged out of the channel and quickly solidified leaving distinct boundaries that define each pancake [24-25]. Figure 6 shows a discharge channel from which the molten material is ejected, as result of greater energy input. The relatively large holes in the center of the pancake suggest that there are strong discharges and such holes may penetrate deep into the coating thickness. The discharge channel is shown to be surrounded by solidified material and some localized micro-cracks which may form as result of a rapid cooling by the electrolyte. Where stronger discharges have greater energy inputs which causes a larger amount of substrate and its oxide to melt down, and eventually the molten material is ejected onto the surface, forming larger ceramic particles when it is immediately cooled by the electrolyte. Some microcracks appear on the coating surface: which could be produced by the thermal stresses during the rapid solidification of the molten oxide product in the strong discharge channels [26]. The molten oxides around the pores indicate that the instantaneous temperature in the micro discharge zone might reach several thousand degrees. The surfaces of other coatings were dominated by many randomly arranged curly projections.

Pores of different size are evident on the surface and their sizes reflect the strength of the discharges. Since the creation of porosity cannot be prevented during the PEO process, it is important to find ways to keep the pores as small as possible as well as producing as uniform as possible layers. However, the density of these holes has been reported to decrease substantially with increasing process time [14,27]. The pore size in the coatings varies from 0,01 to a few μm [14]. Furthermore, there are also many very small holes (micro-pores) in the surface, which are due to gas bubbles ejected from surface discharges as shown in Fig. 7(a,b). If necessary, the porosity can be decreased by proper adjustment of the current mode and density, or/and impregnation by various materials. For example, the bipolar and unipolar current modes for the PEO coating of a AJ62 magnesium alloy have been compared and it has been shown that the use of a bipolar mode can reduce the pore density and size, as well as other coating defects [28]. Although a porous microstructure may be beneficial as lubricant reservoir to decrease wear, and for biocompatible applications where it is beneficial for the rapid adhesion and growth of cells, resulting in a significantly stronger bond to the parent tissue [29], it will also result in a decrease in corrosion resistance of the PEO coatings. The surface roughness also increases as the coating thickens. The actual roughness depends on the particular alloy and the treatment parameters.

As the PEO coating thickens, the evolving micro discharges continuously affect the sintering, crystallization and phase transformations in the coating. The PEO coatings are generally described as a multilayer system. Fig. 7(c-d) illustrates the structure of a typical PEO coating (example is for a Mg-alloy). The coating is composed of three layers namely: a porous outer layer, intermediate dense layer and thin inner dense layer. Coating thickness can range from few to more than 200 microns. However, it should be noted that the PEO layer is partly growing into the original substrate surface and is partly built-up on top of it. Coating growth rate, relative sizes, structure and composition of their different regions are greatly influenced by substrate composition, electrolyte composition and current operating modes and magnitude [3,30,31].

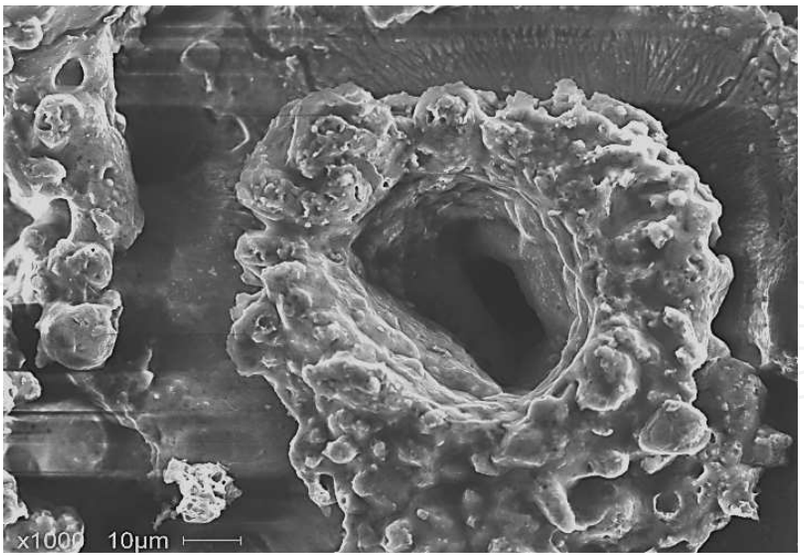

Figure 6. SEM image of a discharge channel; a typical feature of PEO coating processed for 60 minutes at current density of 0.15 A/cm2. Such a pore may penetrate the entire coating thickness to the substrate.

Nie et al [32] studied the microstructure of the inner layer, near the coating/substrate interface, using cross-sectional TEM (Fig. 8). This layer exhibits a number of (predominately amorphous) sub-layers, whilst the lower portion of the intermediate layer has a nano-scaled polycrystalline microstructure. The characteristics of the coating near the interface with the Al 6082 alloy substrate can be divided into hree sub-layers (1, 2 and 3 in Fig. 8(a)).

The PEO coatings on Mg alloys present a porous outer layer, intermediate (or compact) inner layer and dense coating/substrate interface with minimum porosity. The coatings are comprised of amorphous and crystalline phases such as MgO, Mg_2SiO_4, $Mg_3(PO_4)_2$ or Mg_2AlO_4, depending on the different electrolyte [15,33-34]. A typical XRD profile showing the results of phase composition analysis performed on PEO coatings on AZ91 magnesium alloy by Lee et al [35] in three different electrolytes (Bath A contains 0.09 mol/l KOH, 0.5 mol/l KF, 0.1 mol/l $K_4P_2O_7$, Bath B contains an extra 9 g/l ZrO2 while Bath C contains an extra 9 g/l TiO2), is presented in Fig. 9.

Previous work [32,36] had also shown some porous areas near the interface of MgO and Al_2O_3 coatings on Mg and Al substrates using transmission electron microscopy (TEM) [32]. The Al_2O_3 coating was however demonstrated to have superior mechanical and wear properties [32]. On the other hand, such a porous region was not observed in a TiO_2 coating on Ti6Al4V alloys after the PEO process [37].

For the PEO coatings on Al alloys, the porous outer layer consists predominantly of the low temperature modification of alumina, γ-Al_2O_3, with poor mechanical properties. The dense inner layer, on the other hand, is comprised of the mixture of high temperature α- Al_2O_3 modifications of Al_2O_3 and complex Al-X-O phases (X is an element from the electrolyte eg. Si, P), where complex phases of the substrate alloying elements are observed in a thin, interfacial region below the dense layer. The content of the α- Al_2O_3 phase is increased with increasing coating thickness, which may be attributed to the following two reasons. First, any

http://dx.doi.org/10.5772/57171

phase transformation takes place when the discharges are strong enough to heat the oxide coating to the required temperatures, for a time adequate to allow phase transformation. Second, internal residual stresses will be formed as result of the rapid heating and cooling cycles experienced during coating formation. The formation of stable α- Al_2O_3 is favored by relief of these stresses [30]. The aluminum oxide coating morphology and microstructure were also significantly different under different current operating modes [33, 38]. The bipolar current mode could improve the coating quality compared with the unipolar current mode, in terms of surface morphology and cross-sectional microstructure. A dense coating morphology could be achieved by adjusting positive to negative current ratio and their timing to eliminate or reduce the strongest plasma discharges [39]. PEO coatings have excellent adhesion with substrate, which is due to a transition layer on the interface. The transition layer is growing both inside the substrate, and outside, as a result, the coating is integrated with the substrate.

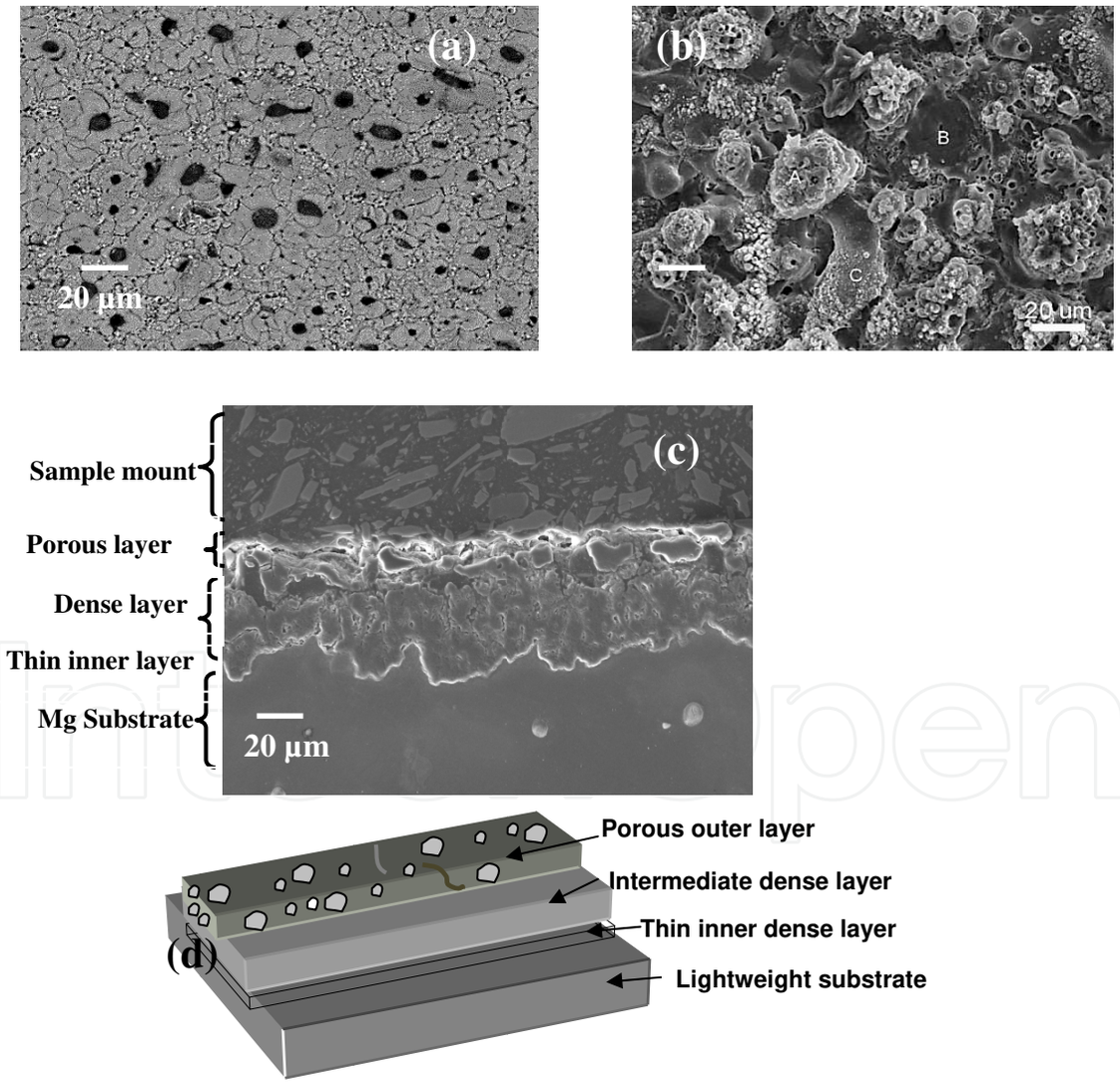

Figure 7. SEM micrographs showing (a,b) the surface morphology, (c) cross-section of PEO coating on AM60B alloy and (d) illustration of the coating layers of PEO coatings.

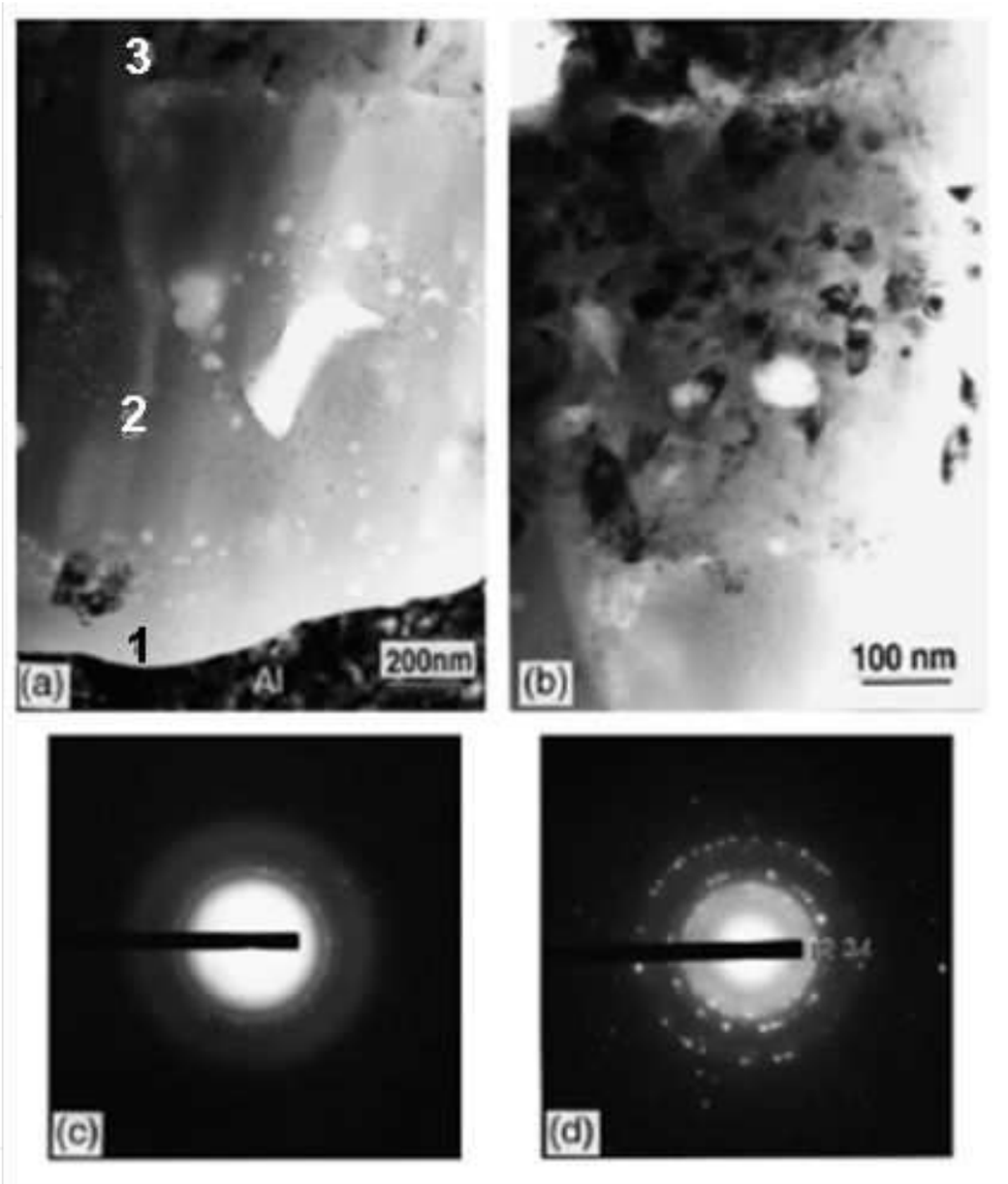

Figure 8. Cross-section TEM images of Al 6082 substrate of (a) the inner layer near coating/substrate interface and (b) the intermediate layer, and SAED patterns taken from intermediate (c) sublayer 2 and (d) sublayer 3, respectively [32].

The effect of the substrate chemical composition on phase evolutions in the PEO coatings formed has been investigated [4, 26, 39]. It has been shown that the amount α-Al_2O_3 phase can be substantially increased, reaching 60 % or more, for coatings produced on aluminum alloys containing 4 – 5 % Cu [4]. Such high fractions of the α- Al_2O_3 phase is generally regarded as responsible for the high hardness, up to 16–25 GPa [26], and low bulk stiffness, of PEO coatings which makes them attractive for wear protection. However, the electrolyte composition is a key factor in promoting any specific phase formation. For instance, it has been shown that, sodium aluminate ($NaAlO_2$) in the electrolyte can be, at least partly, responsible for the formation of more α-alumina [38].

http://dx.doi.org/10.5772/57171

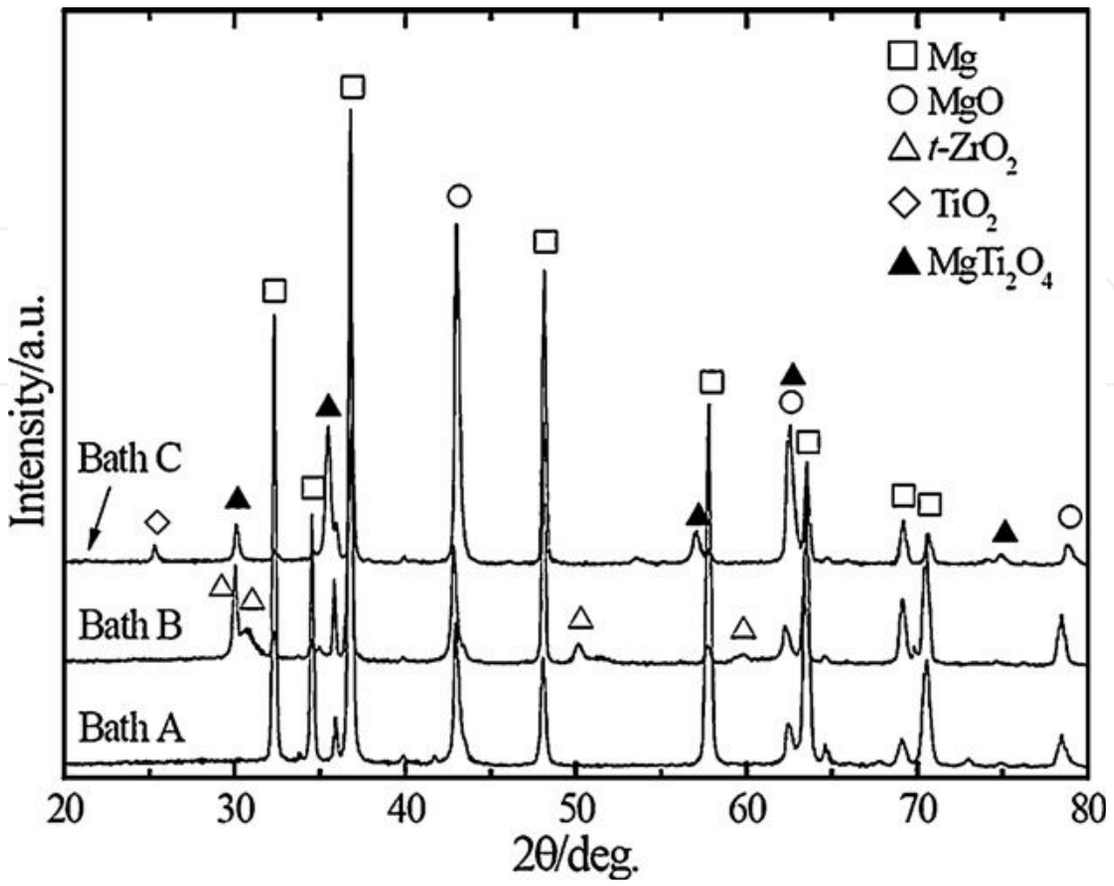

Figure 9. Qualitative XRD patterns of the oxide layers of AZ91 Mg alloy coated in different electrolytes [35].

6. Coating formation mechanisms

6.1. Electrochemistry of plasma electrolytic oxidation (PEO)

The growth of the oxide coating mainly occurs due to three different, yet simultaneous, processes, namely: the electrochemical reactions, the plasma chemical reactions [40-42] and thermal diffusion. The electrochemical formation of surface oxide layers can occur through different mechanisms depending on the electrolyte, eg. silicates, aluminates, phosphates. The PEO coatings are usually produced by AC or bipolar current mode, containing both anodic and cathodic components. An early investigation of the basic electrochemical processes of AC PEO coatings on Ti, has been carried out by Yerokhin et al [43] using AC current mode and a complex aluminate-base electrolyte. According to their study an oxide layer formation is induced both by the ionic component of the current which is transmitted via surface discharges and by the anodizing current passing across the surface which is free of discharges (Figure 10). The other components of the current cause secondary electrochemical processes which lead to liberation of electrode gases (H_2 and O_2) and anodic dissolution of the titanium metal as shown in Figure 10, where the following general reactions normally occur:

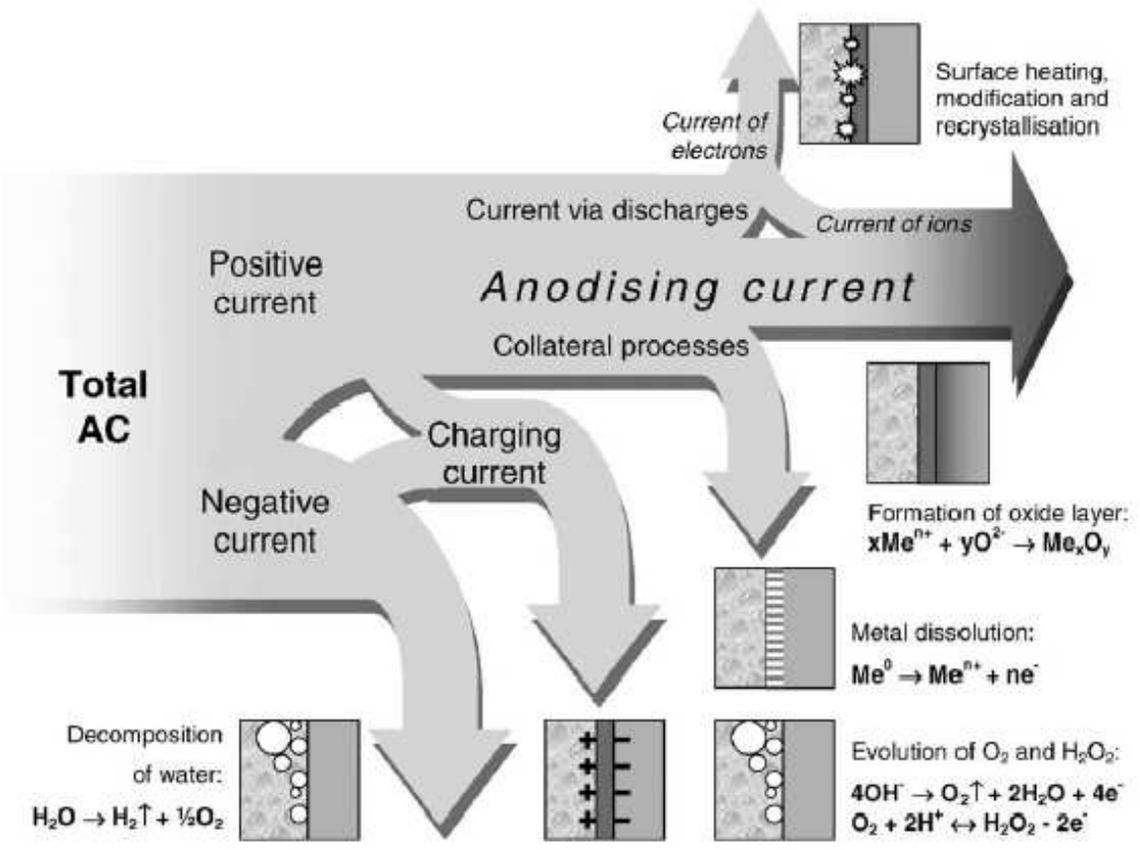

Figure 10. Schematic diagram of current distribution during the PEO treatment of metals in AC mode [43].

- Metal-oxide interface:

$$Ti \longrightarrow Ti4+ +4e- \tag{1}$$

For alkaline aluminate solutions the anions (OH- and AlO2-) can take part in the following processes on the oxide/electrolyte interface [43,44]:

$$Ti4+ +4OH- \longrightarrow TiO2 +2H2O \tag{2}$$

$$Ti4+ +4AlO2- \longrightarrow TiO2 + Al2O3 \tag{3}$$

$$Ti4+ +Al(OH)4 - \longrightarrow TiO2 + Al2O3 + 2Al(OH)3 + 5H2O \tag{4}$$

Dissolution and oxygen evolution is quite common in aluminum PEO in alkaline solutions, where the following general reactions normally occur [30]:

- Metal-oxide interface:

i. anodic processes:

$$2Al + 3O^{2-}_{solid} \rightarrow Al_2O_3 + 6e^- \quad (5)$$

$$Al \rightarrow Al^{3+}_{solid} + 3e^- \quad (6)$$

- Oxide-electrolyte interface

i. anodic process

$$4OH^- \rightarrow O_2 \uparrow + 2H_2O + 4e^- \quad (7)$$

ii. alumina chemical dissolution and oxidation of ejected Al:

$$Al_2O_3 + 2(x-3)OH^- + 3H_2O \rightarrow 2[Al(OH)_x]^{n-}_{gel} \quad (8)$$

$$Al^{3+}_{ejected} + xOH^- \rightarrow [Al(OH)_x]^{n-}_{gel} \quad (9)$$

$$[Al(OH)_x]^{n-}_{gel} \rightarrow Al(OH)_3 \downarrow + (x-3)OH^- \quad (10)$$

It has also been found that the film growth rate decreased significantly with increasing electrolyte concentration, since the rate of anodic dissolution increased.

For magnesium alloys the main electrochemical reactions occurring at the metal/oxide and oxide/electrolyte interfaces are as follows [10,15]:

- Metal-oxide interface:

$$Mg \rightarrow Mg^{2+} + 2e^- \quad (11)$$

$$4OH^- \rightarrow 2H_2O + O_2 \uparrow + 4e^- \quad (12)$$

- Oxide-electrolyte interface:

$$Mg^{2+} + 2OH^- \rightarrow Mg(OH)_2 \quad (13)$$

$$Mg(OH)_2 \rightarrow MgO\downarrow + H_2O \tag{14}$$

$$Mg^{2+} + 2AlO_2^- \rightarrow MgAl_2O_4\downarrow \tag{15}$$

$$2Mg^{2+} + SiO_3^{2-} + 2OH^- \rightarrow Mg_2SiO_4\downarrow + 2H_2O \tag{16}$$

$$3Mg^{2+} + 2PO_4^{3-} \rightarrow Mg_3(PO_4)_2\downarrow \tag{17}$$

Reaction (11) is the anodic dissolution and (12) is the oxygen evolution reaction. The cation released from the metal (reaction (11)) combines with the anion in the electrolyte to form compounds $Mg(OH)_2$, Mg_2AlO_4, Mg_2SiO_4 or $Mg_3(PO_4)_2$, depending on the different electrolyte by reactions (13), (15), (16) and (17). The unstable hydroxide $Mg(OH)_2$ dehydrates to MgO by the high temperature (reaction (14)), resulting from the plasma discharge.

6.2. Plasma discharge models and plasma chemistry

Several micro-discharge formation models have been proposed [45-49]. In the first model [46], the micro-discharges appear as a result of the oxide film dielectric breakdown in a strong electric field. The second group of models considers each microdischarges as a gas/glow discharge occurring in a micropore of the oxide film [47]. The formation of a gas phase in the pore (and discharge ignition in it) is believed to be induced by an initial dielectric breakdown of a barrier layer in the bottom of the micropore [45]. The third model [49] assumed the possibility of free electron generation and glow discharge ignition in the gaseous media at the oxide-electrolyte interface, which leads to heating, melting and quenching the underlying oxide layer. Any other model considers the formation of the micro-arc discharge as an electronic 'avalanche', or due to an electronic tunneling effect [48]. Yerokhin et al [45] found that the above models [46-49] do not fit the spatial, temporal and electrical characteristics of microdischarge phenomena which were observed in their investigation. They suggested a new model based on the analogy with contact glow discharge electrolysis. The model assumes the possibility of free electron generation and glow discharge ignition in the gaseous media at the oxide-electrolyte interface, which leads to heating, melting and quenching of the underlying oxide layer.

Recently, optical emission spectroscopy (OES) has been used to investigate the plasma discharge behavior during the PEO process [4,33]. Species from the substrate (Mg, Al and Ti) and the electrolyte (H, OH, Na and K) were found to be involved in the plasma discharge during the PEO process. The evolution of the spectra is considered to reflect the change in mechanism that initiated the plasma discharge, from bound-bound transitions of electrons between atomic level to collision–radiative recombination of electrons (bound-free transitions) and Bremsstrahlung radiation (free-free transitions). According to Dunleavy et al [33], the plasma emission spectra indicated that there were two distinct regions of the plasma, a central

http://dx.doi.org/10.5772/57171

core of high temperature (~16, 000 ± 3500 K), with a high electron density (N_e ~5× 10^{17} cm^{-3}) and a peripheral region, probably extending into the surrounding electrolyte, which was much cooler (~3000-4000 K) and less dense (N_e ~5× 10^{15} cm^{-3}). Hussein et al studied the evolution of the emission spectra of plasma discharge during the PEO process [39]. The fluctuations in plasma intensities and temperatures during the plasma discharging as well as the coating morphology were found to be due to the different types of discharge, which originated at the metal/coating interface (type B), within the coating upper layer (type C), or at the coating surface/electrolyte interface (type A) [4]. Type B discharges are responsible for the high temperature spikes (up to 10 000K) present in the electron temperature profiles. On the other hand, type A and C discharges produce the base temperature profile and any small fluctuations around this base line (~ 4500K).

Hussein et al. [10] have described the coating development during PEO processing based on a general theory of the breakdown of a metal/dielectric system in an electric field, optical emission spectroscopy observations and SEM/EDX analysis of the coatings. Their general coatings mechanisms can be applied to the PEO processing of any of the light-weight metals (Mg, Al, Ti or Zr). However process parameters including electrolyte composition or electrical parameters (DC, AC, unipolar, bipolar, constant current or voltage) have a significant effect on such mechanisms. Figure 11 is a schematic of a PEO coating process on a magnesium substrate. For PEO an appropriate electrical potential is applied to substrate to increase the thickness of the thin oxide layer on the surface of the alloy which could provide a very limited protective effect (Fig. 11(a)). As the surface has been passivated by a non-conductive oxide coating, the voltage between the substrate and the electrolyte rapidly rises as the native oxide thickens (Fig 11(b)) and within a few minutes the voltage reaches several hundred volts. The voltage increases until it has become too high for the dielectric coating and a microscopic plasma discharge breaks the coating and generates a large number of very short-lived, very small plasma discharges (Fig 11(c)). These discharges result in localized plasma reactions, with conditions of high temperature and pressure which modify the growing oxide. This break-down results in the formation of a slightly thicker coating, which will be broken again in the course of the next cycle, under a slightly higher potential difference. During the process, the number of discharges decreases but their intensity increases.

An important consequence of the occurrence of those discharges is the development of metallurgical processes in the growing oxide layer, which are induced by the heat liberated in discharge channels from the electron avalanches. Because of the local high temperature ~10^4 K [4,50] and the strong electric field, of the order of ~ 10^6 V/m [3], molten oxide is ejected from the discharge channels in the coating/substrate interface into the coating surface where it is rapidly solidified and re-crystallized by the electrolyte, Fig 11(d). As a result, decomposition of metal hydroxide to oxide and formation of complex compounds can occur, Fig 11(e). The intensity of these processes depend on the density and power of the discharges which are known to be defined by thickness of the oxide layer. Therefore, the thicker the layer, the less frequent, yet more powerful and extended, the discharges become [10].

As shown in the schematic diagram Fig. 11(b), the metal cations that transfer away from the metal substrate react with anions to form a ceramic coating. On the other hand, oxygen anions

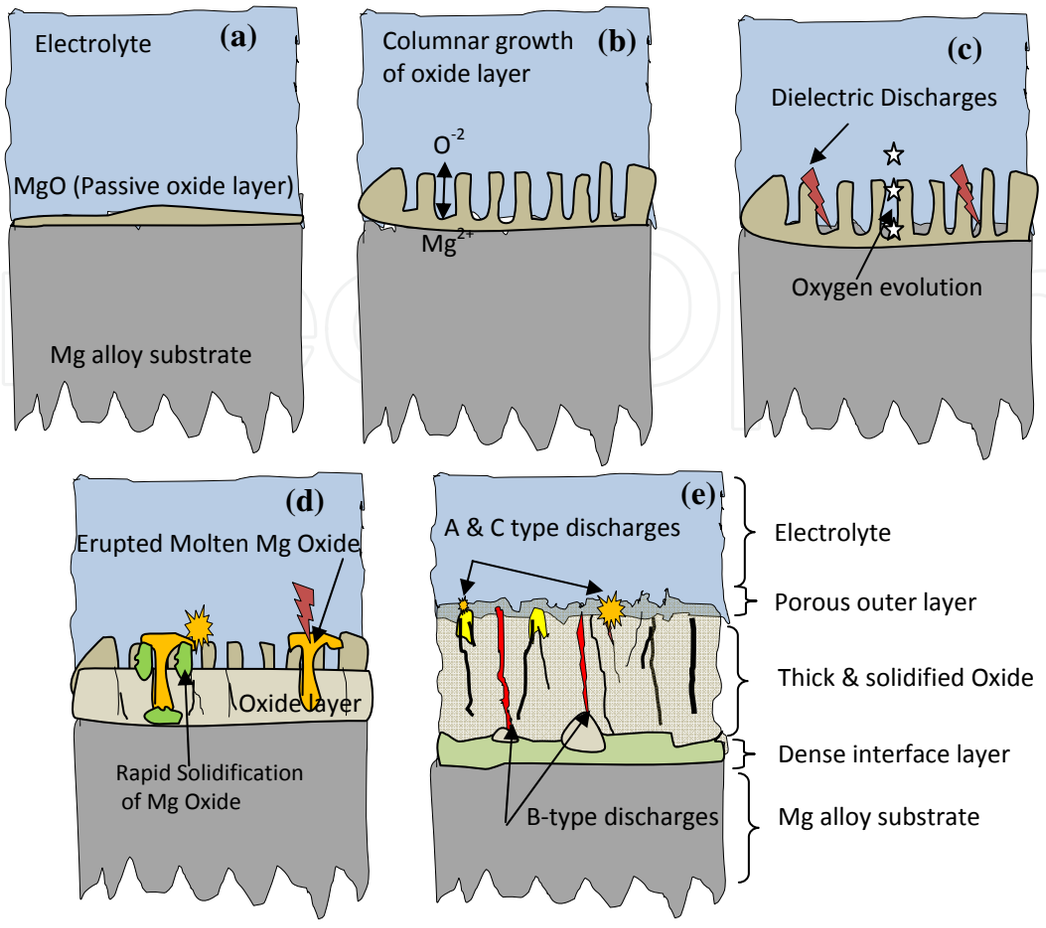

Figure 11. Schematic of coating development during PEO processing.

transfer into magnesium substrate due to the high electric field in the discharge channels and react with Mg^{2+} cations to form a ceramic coating. The instantaneous high temperature and high pressure in the discharge zone greatly enhances inter-diffusion between the oxygen anions and magnesium cations in the coating near the discharge zones. At higher plasma temperatures, the thermal energy supplied to the diffusing ions (O^{2-}) allows the ions to overcome the activation energy barrier and more easily move and interact with the magnesium cations Mg^{2+} produced during the discharges to form MgO.

7. Growth mechanisms

The plasma chemistry of the surface discharges is quite complex in nature, involving, on one hand, charge transfer at the substrate/electrolyte interface, and on the other hand, strong ionization and charge transfer effects between the substrate surface and the electrolyte through the oxide layer with the aid of the plasma [10,51]. Generally, the discharge event tends to occur in the coating–substrate interface or regions near the interface, which are responsible for the thermal and chemical conditions at the metal surface, thus playing an important role in

http://dx.doi.org/10.5772/57171

formation, composition, and structure and stress state of phases formed. However, it is worth mentioning that the discharges induce no changes of substrate microstructure or texture. Processes such as melting, melt-flow, re-solidification; sintering and densification of the growing oxide take place during the PEO coating process.

1. **Linearity of the growth rate:** Most PEO studies indicate that the coating thickness increases linearly with coating time [31,52]. However, some research [41,53] shows that such linearity could break down at longer treatment times. According to Sundararajan et al.'s proposed growth mechanism [31,52], the growth of oxide layers results only from molten substrate elements which are oxidized when flowing out through the discharge channels that are created due to the oxide layer breakdown. In this way, an oxide is formed which contributes to the layer when being ejected from the channels and rapidly cooled at the surface–electrolyte interface. Discharge channels are continuously formed and move on the coating surface and since they have a finite life, they are formed and closed continuously through the coating process and contribute to the coating thickness.

2. **Inward and outwards coating growth:** Xue et al [41] describe the growth mechanism of the ceramic coating layer as a combination of inward inwards to the alloy substrate (inner layer) and outwards to the coating surface (outer layer) simultaneously. Fig. 12 is a schematic diagram of the coating development during PEO. The dashed line between Lo and Li in Fig. 12 represents the position of the original surface of the substrate before PEO treatment. During the early stages, the coating grows mainly outwards. After the coating reaches a certain thickness the inner layer grows faster than the outer layer. However, at this time, the coating thickness continues to increase in both directions. The inner growth is attributed to the growth of the compact layer at the film/substrate interface by diffusion or transport of oxygen, while the growth of outer layer onto the surface are due the electrochemical and the plasma chemical reactions.

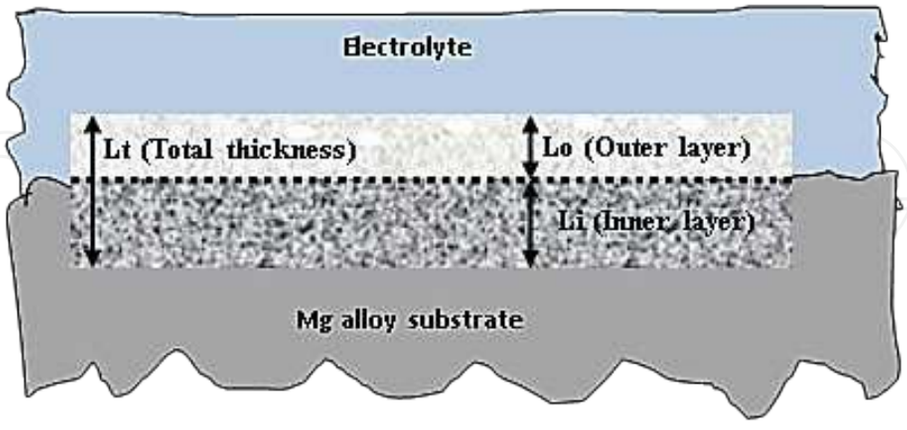

Figure 12. Schematic diagram of dimension changes of magnesium alloy before and after PEO treatment.

3. **Growth of compact layer at film/substrate interface by diffusion or transport of oxygen:** At longer processing times, the inward coating growth rate increases. This change may be connected to the increase of thermally-activated diffusion. For PEO process, both

thermally-activated diffusion and ions transformation have an important contribution leading the coating growth [52]. Inward oxygen diffusion plays a key role in coating growth, and the growth rate of the PEO process coating is controlled by the rate of transferring oxygen towards the magnesium substrate as shown in the schematic diagram of Fig. 11(b-e).

4. **Growth rate dependent on the process parameters:** The rates of growth of the outer and inner oxide layers are process parameter dependent. They result from a combination of three processes namely, (i) discharge processes causing the substrate to melt and oxidize when flowing out through the discharge channels and being rapidly cooled at the surface–electrolyte interface, (ii) partial destruction of the outer layer due to strong discharges and (iii) diffusion of oxygen process from the electrolyte towards the substrate through the coating.

8. Corrosion protection afforded by PEO coatings

8.1. Mg-alloys

Magnesium and its alloys have gained increasing attention for applications requiring high strength to weight ratio, high thermal conductivity, excellent castability, and ease of recycling. However, magnesium alloys exhibit very poor corrosion resistance caused by their chemically active nature, especially galvanic corrosion [2], which can further cause severe pitting corrosion on the metal surface resulting in decreased mechanical stability and an unattractive appearance.

Song and Atrens have concluded that internal galvanic attack, due to potential difference between matrix and precipitates, and the instability of the magnesium hydroxide film formed on the surface of Mg alloys are the two main causes for corrosion of magnesium alloys [54]. When magnesium is exposed to an aqueous solution, both $Mg(OH)_2$ and MgO can be formed: $Mg(OH)_2$ is in contact with the metal, and on top of the hydroxide layer is a MgO layer that has direct contact with the aqueous solution. For pure Mg, this layer is not protective at pH values below 10.5, unless additional alloying elements are added to pure Mg. The corrosion mechanism for the Mg alloys is more complex than that for pure magnesium, due to a multi-phase microstructure. Shi et al [55] pointed out that corrosion rate of Mg alloys is strongly dependent on the composition of the α-Mg matrix and the distribution of the other phases. Such phases have the tendency to accelerate the corrosion of the α-phase. In order for a coating to provide adequate corrosion protection for Mg and Mg alloys, the coating must be uniform with minimum defects and pores and well adhered.

Coating surface morphology, porosity, structure and corrosion behavior of ceramic coatings on Mg-alloys, are affected by many parameters including, electrolyte composition and concentration, the substrate composition, and the process parameters (including current density, current mode, applied voltage, temperature, and treatment time [10]. Test methods most commonly used to determine a corrosion rate of the PEO coatings are immersion tests, potentiodynamic polarization studies and impedance spectroscopy (EIS) [56].

http://dx.doi.org/10.5772/57171

Immersion testing is the most frequently conducted test for evaluating the corrosion of metals in aqueous solutions and can be used for evaluate the resistance of the metal to pitting, crevice corrosion and galvanic corrosion. It is basically depends on total immersion of a test specimen in a corrosive solution for a period of time and then immediately examining it. The electrochemical technique of Tafel extrapolation of polarization curves is also widely used for the evaluation of the corrosion of Mg alloys, in particular coated Mg alloys, because it is simple and fast. Atrens and co-workers [57] have raised a number of issues concerning the reliability of the Tafel extrapolation technique for corrosion measurement of Mg and Mg alloys, and therefore, suggest that Tafel extrapolation should be used with appropriate caution. Electrochemical impedance spectroscopy (EIS) can provide valuable information about surface treatment layers on PEO-coated magnesium, and the interfaces between electrolyte/coating/substrate [10]. It also allows the kinetics of heterogeneous electron-transfer reactions, coupled chemical reactions, or adsorption processes to be studied, and can provide information about pitting and crevice corrosion [58].

Corrosion studies have been mainly performed in aqueous NaCl solutions which can simulate natural seawater of any specified salinity, or in Hanks solution or simulated body fluid (SBF) for biocompatibility studies [59]. Zhang et al. [60] were the first to use Hanks solution to study the corrosion behaviour of PEO-treated Mg alloy samples, followed by Xu et al [61]. All PEO coatings reduced the corrosion rate to a certain extent. However, longer exposure of the PEO coated samples to an aggressive medium will minimize the protection process due to the defects and open pore structures of the PEO layers. Defects always exist as a result of many factors including: discharging process, solidification process, mechanical stresses, and gas evolution during the process. Figure 13 shows the effect of different PEO treatment time on the corrosion properties of AZ91D Mg alloy in 3.5%NaCl solution [62]. The potentiodynamic results show that the corrosion current density (icorr) decreased with PEO processing time. However, the corrosion potential (Ecorr) was relatively constant. The EIS results revealed that ~2 orders of magnitude higher resistance of the inner layer, mainly contributed to the overall resistance of PEO coating.

Using potentiodynamic polarization curves and electrochemical impedance spectroscopy, Barik et al studied the corrosion performance of PEO coatings, and demonstrated that unsealed PEO coating allows permeation of the solution through the pores in the coating [63]. The corrosion rate of the various magnesium alloys coated using either the PEO method and composite polymer-containing coatings has recently, been investigated by Gnedenkov et al [64] using a scanning vibrating probe method (SVP). The SVP method allows the study of the changes in the electrochemical activity of the sample on a micro scale and is particularly useful in investigating the effect of the alloy composition and microstructure on corrosion behavior [62,64-65]. According to their analysis of the SVP data, they conclude that the secondary phases in a VMD10 Mg alloy have a greater effect than α-phase on the corrosion behaviour and accelerate the dissolution of the α-phase.

Comparison of the corrosion protection results offered by PEO is very difficult, due to the variation of the experimental test parameters including solution composition, concentration, test time and other parameters. Ma et al. reported that oxide films grown on a AM50 magne-

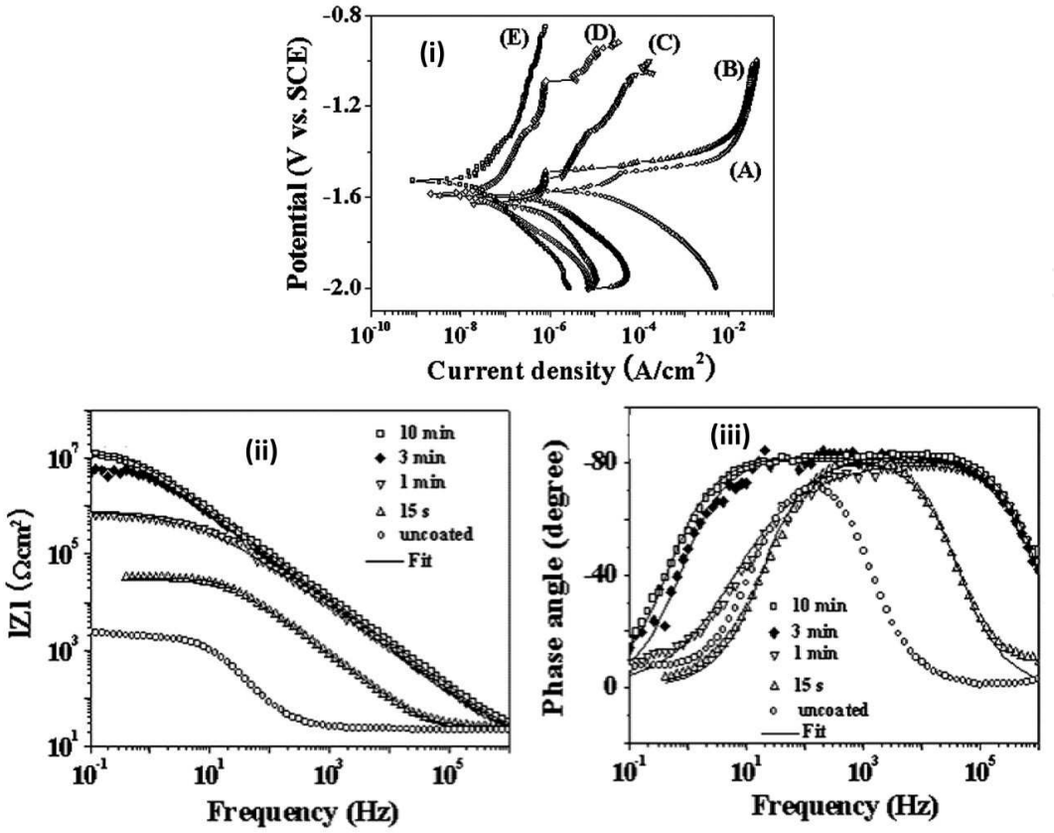

Figure 13. (i) Potentiodynamic polarization curves and (ii and iii) Bode plots of (A) uncoated AZ91D Mg alloy and PEO coatings treated for (B) 15 s, (C) 1 min, (D) 3 min, and (E) 10 min in 3.5 wt.% NaCl solution [62].

sium alloy from a phosphate solution have better corrosion resistance [66] compared with coatings prepared in silicate solutions. However, Liang et al. [67] when comparing the PEO coatings on AM60B magnesium alloy formed in silicate and phosphate electrolytes concluded that PEO coatings produced in a silicate electrolyte are compact and uniform hence exhibit better corrosion resistance thus coatings formed in a phosphate electrolyte, which were relatively porous. Liang et al [68] investigated the electrochemical degradation of a silicate- and phosphate-based PEO coatings on a AM50 magnesium alloy using a pulsed DC power supply in NaCl solutions of different chloride ion concentrations (0.01, 0.1, 0.5 and 1 mol/L). They conclude that the corrosion resistance of the Si-PEO coating was superior and the corrosion deterioration was slower than that of the P-PEO coating in mild corrosive electrolytes (0.01M and 0.1M NaCl). However, in the more concentrated electrolytes (0.5M and 1M NaCl), the Si-PEO and P-PEO coatings cannot provide a long-term protection to the magnesium alloy substrate due to the initiation of localized corrosion, and undergo further deterioration. Ding et al [69] investigated the influences of the addition of Na_2WO_4 to the silicate based electrolyte and breakdown voltage on the PEO coatings microstructure, hardness and wear resistance. In the presence of Na_2WO_4, the coatings have excellent compactability and wear resistance. However, with increasing sodium tungstate concentration, the size of micropores in the PEO coatings prepared in the NaOH electrolyte increased and the corrosion resistance of the PEO coatings decreased [70]. Figures 14 (a,b) show the effect of electrolyte additives (shown in Table

http://dx.doi.org/10.5772/57171

3) on the corrosion performance of PEO coatings formed on magnesium alloy AZ91D [15]. The potentiodynamic polarization results show that the coatings made using electrolyte P had a relatively lower Tafel slope due to a thinner coating with more micro-defects than those made using B- or M solutions. The coating with the M-electrolyte had the highest Tafel slope, which was attributed to a thicker, uniform structure and compact inner barrier layer formed in the bath with additions of fluoride and borate. The different EIS behavior (corrosion resistance) of the PEO films was attributed to their different structures and chemical composition.

Composition (g/l)	Solution P	Solution B	Solution M
$Na_2SiO_3 \cdot 9H_2O$	10–20	10–20	10–20
KOH	3–8	3–8	3–8
$NaH_2PO_4 \cdot 3H_2O$	4–8	N/A	N/A
$Na_2B_4O_7 \cdot 10H_2O$	N/A	5–10	5–10
KF·2H2O	N/A	N/A	5–10

Table 3. Electrolyte composition for PEO processing of magnesium alloy AZ91D [15]

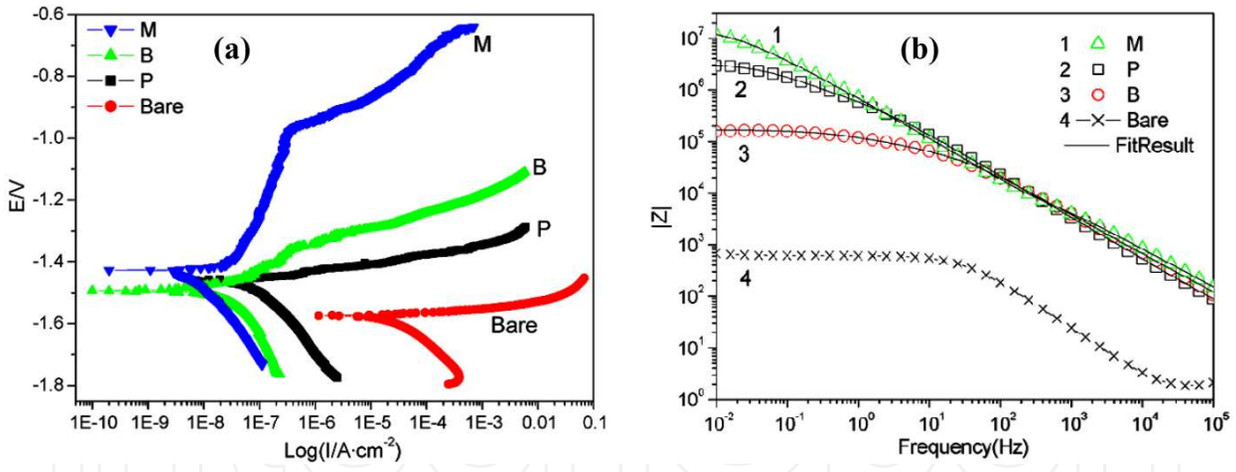

Figure 14. a) Potentiodynamic polarization curves (b) EIS plots of PEO films on AZ91D Mg-alloy treated in solutions containing different additive [15].

Hussein et al [28] studied the PEO-coating corrosion resistance for AJ62 Mg-alloy using both electrochemical impedance spectroscopy (EIS) and potentiodynamic polarization measurements in 3.5%wt NaCl solution. In this study the use of two different current modes (unipolar and bipolar current modes) in sodium aluminates electrolytes for 45 minutes treatment time, were successfully improve the corrosion resistance of AJ62 compared to the uncoated alloy. However, the coating made using the bipolar current mode is more beneficial in improving the corrosion resistance of the PEO coating than the unipolar current mode, see Table 4.

Sample	Current mode	C_R	R_p (Ω·cm²)	EIS R_{total} (Ω•cm2)
S1	Unipolar	N/A	4.10E+04	3.94E+04
S2	bipolar	0.74	1.24E+06	2.80E+06
S3	bipolar	0.63	1.19E+06	1.80E+06
S4	bipolar	1.0	4.72E+05	2.35E+05

Table 4. PEO Process parameters for coating depositions on AJ62-Mg alloy and the corrosion resistance results from both potentiodynamic polarization (R_p) and EIS test (R_{total}) [28].

The use of a bipolar current mode results in the formation of a dense (minimum defects) coatings with higher corrosion resistance compared to coatings obtained using a unipolar or DC mode. Arrabal et al [71] conclude that the AC PEO coating on Mg alloys reduces the corrosion rate by 2-4 orders of magnitude compared with uncoated alloys. Ma et. al. [66] showed that an enrichment of the $MgAl_2O_4$ spinel phase in the coating, together with the minimum amount of cubic MgO, improves the corrosion resistance of the coating. The study of Barchiche et al [72] shows that increasing the treatment time rather than current density will improve corrosion resistance of the PEO oxide layer on AZ91D as well as a more passive behaviour of anodized layer was obtained with the higher concentrated electrolyte (3M KOH) due to the formation of more compact layer with minimum defects. In a review paper by Gu et al [56], a comparison of the results obtained using immersion tests of Mg and Mg alloys showed that PEO coatings were more effective in terms of corrosion protection than other coatings including alkaline and fluoride treated surfaces and organic based coatings. Hussein et al [12] in their review paper compared the corrosion protection affected to a AZ91D Mg alloy by PEO coatings, see Table 5. A close examination of the data shows a considerable variation in the corrosion current density i_{corr}, which is not directly related to the coating thickness. Other studies have demonstrated the practicality of using PEO coatings as a pre-treatment, followed by a second different coating process to seal any pores and cracks formed during the PEO coating process [56,62]. A number of sealing methods have been used for this purpose including: sealing in an organic polymer and sealing by the use of sols. The use of organic based coating, Sol-gel TiO_2 coating, immersion in SBF and electrophoresis deposition (EPD) of calcium phosphate–chitosan coatings on the top of PEO coatings on pure Mg and Mg alloy shows further improvement of the corrosion resistance compared to the PEO coating on its own [73]. A porous structure of the PEO coating is necessary for such treatment to be effective. Fig. 15 shows that the percentage reduction in corrosion rates of magnesium alloys with different coatings reported in the literature compared with uncoated samples [56]. The reported reduction in corrosion rate using a polymer coatings (chitosan coatings [78], poly-caprolactone and dichloromethane coatings [77]), electrodeposition coatings (dicyclopenta-diene (DCPD), hydroxyapatite (HA) and fluoridated hydroxyapatite (FHA) coatings [76]), fluoride treatment [75] and alkaline heat treatment [74], around 50–80% compared to more than 90% that can achieved using PEO coatings method [56].

Refs.	PEO operational condition		Coating Thickness µm	Corrosion Data		
	Electrolyte	Applied Power		Testing Method	i_{corr} µA/cm²	E_{corr} V
[102]	NaOH 7 g/L, sodium hexametaphosphate 4 g /L and calcium acetate 0.4 g/L	CV, CC,CP 2 Adm^{-2}	3-15	EIS + P.P. In Hanks solution 37,5 °C	2.4	-1.660
[62]	KF 9 g/L + $NaAlO_2$ 10 g/L	DC pulse 5 A dm^2	15	P.P. in 3.5% NaCl solution	0.01	-1.53
[103]	phosphate		10	phosphate	NA	-1.64
[104]	K_2ZrF_6 =10, $Na_2SiO_3{\cdot}9H_2O$= 10, KOH= 4	CV 300v	10	P.P. in 3.5% NaCl solution	0.05	–1.42
[105]	Na2SiO3·9H2O 10–15 g/L, KOH 2–4g/L, KF·2H2O 3–5 g/L, Na2B4O7·10H2O 2 g/l	CV 400v	20-50	EIS + P.P. 3.5% NaCl solution for 220 h,	7.5	–1.41
[106]	NaOH and Na_2SiO_3	Unipolar 400-460v	3-10	P.P. in 0.9% NaCl solution	0.64	_1.49
[15]	$Na_2SiO_3{\cdot}9H_2O$, KOH, $NaH_2PO_4{\cdot}3H_2O$	350–400V	20	P.P. in 3.5% NaCl solution	0.003	–1.43
[107]	NaAlO2 20 g/l and NaOH 8 g/l	30 mA/cm^2	10	galvanic corrosion in 5%NaCl	$1.9x10^4$	NA
[60]	2oog/L CrO_3+10g/L $AgNO_3$	NA	NA	P.P. In Hanks solution 37,5 °C	0.204	-0.430

NA= not available; CV= constant voltage; CC= constant current; CP= constant power; P.P.= potentiodynamicl polarization; icorr= corrosion current density; Ecorr= corrosion potential.

Table 5. Examples of plasma electrolytic oxidation of AZ91D Mg alloy. Adapted from [12].

The studies by Arrabal et al [79] shows the effect of the immersion time and the effect of duplex coating combining PEO and polymer layer on AZ31 magnesium alloy as shown in Figs. 16 and 17. PEO treatment significantly increased the corrosion resistance of the AZ31alloy, but only for short immersion times due to the porous nature of the outer region of the PEO coating and deterioration of the inner barrier layer (Fig. 16). As for the PEO + polymer coated specimens, high impedance values indicated almost negligible degradation of the polymer top-layer after 77 days in 5 wt.% NaCl solution and superior corrosion resistance properties of the PEO pretreatment (Fig 17).

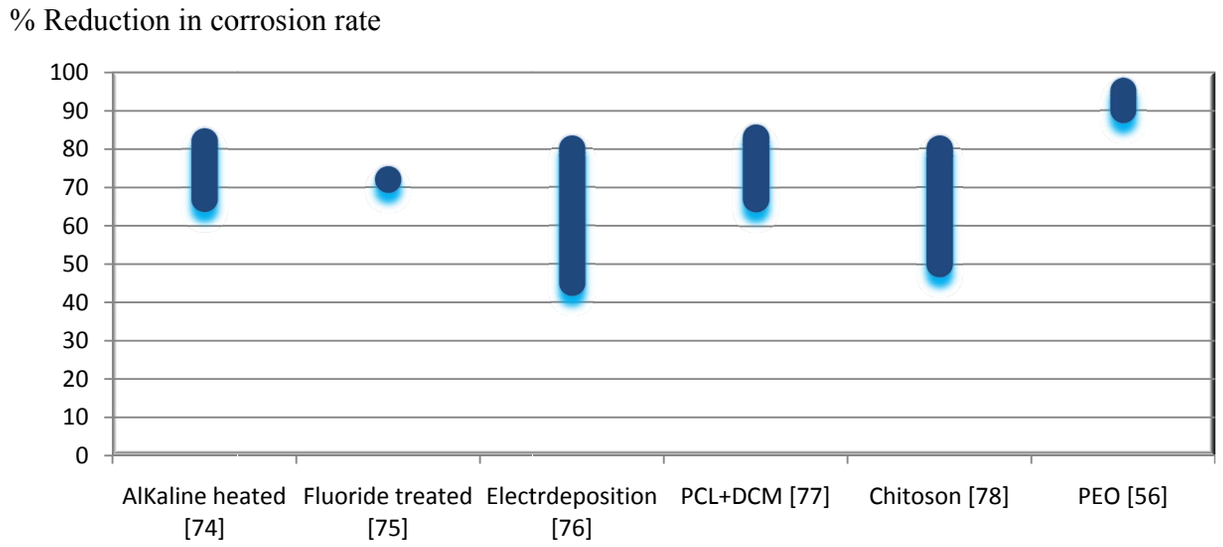

Figure 15. The reduction in corrosion rate for magnesium alloys with different coatings. (adapted from [56]).

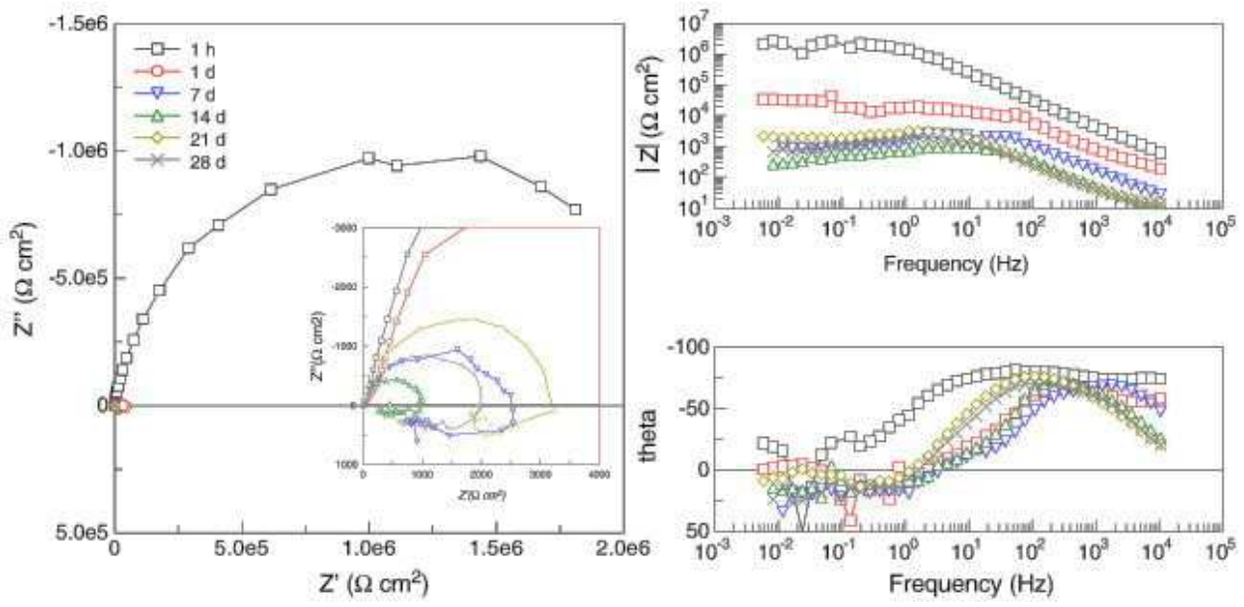

Figure 16. Nyquist and Bode plots of PEO coated AZ31 alloy [79].

http://dx.doi.org/10.5772/57171

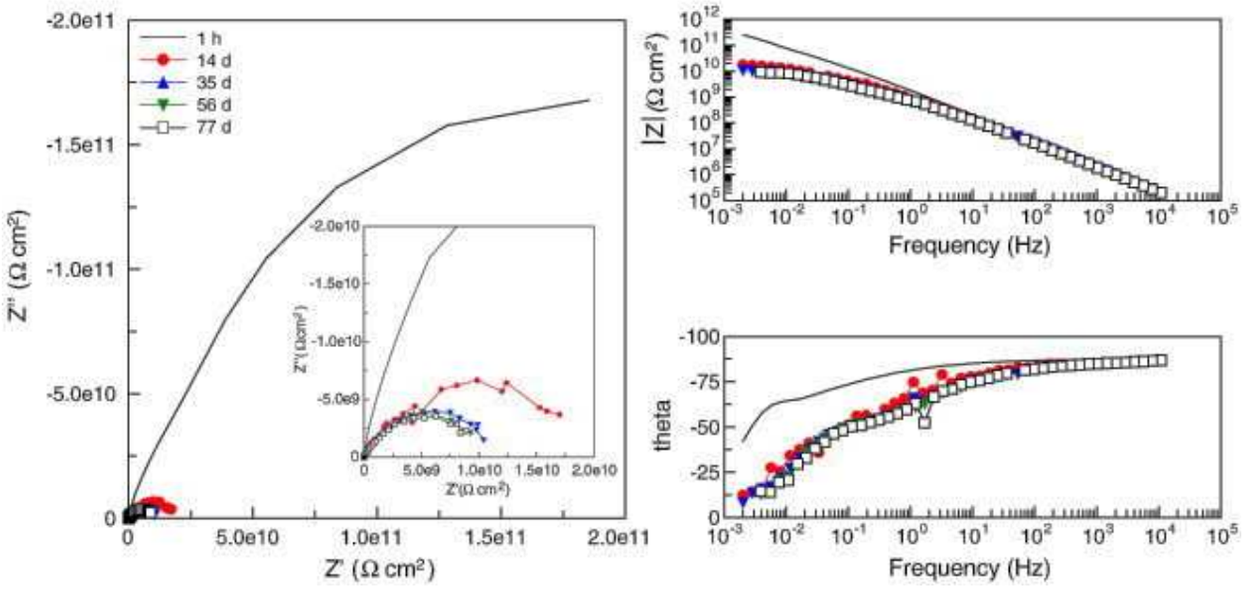

Figure 17. Nyquist and Bode plots of PEO + polymer AZ91 alloy specimen [79].

8.2. Al-alloys

The poor corrosion protection properties of uncoated Al substrates result from the fact that the corrosion resistance considerably decreases after the thin protective oxide film on the uncoated aluminium substrate surface is broken down by the corrosion processes. The corrosion resistance of PEO coatings on aluminum alloys was studied by Nie et al [32], where the effect of thickness on the mechanism and properties of ceramic coatings were measured. They conclude that the PEO-coated 6082 Al alloys exhibited excellent corrosion resistance in 0.5 M NaCl solution, considerably better than even stainless steel. The corrosion protection properties of PEO coated aluminum alloys have been investigated using potentiodynamic polarization curves and electrochemical impedance spectroscopy (EIS) [63,80-81]. The corrosion performance of PEO-coated Al-alloys for long time immersion times can be divided into three stages: (i) the penetration of corrosive medium into aluminum alloy is inhibited effectively by the PEO coating in the initial stage of immersion (less than few hours); (ii) after immersion for more than 10-24 hours, the corrosive medium penetrated into the interface between the alloy and the coating, through the pores and cracks in the coating, and caused corrosion under the coating. Although a similar decreasing trend is observed in the resistance of the compact layer values, they are very high compared with the outer layer values measured for the porous layer at all immersion time.; and (iii) after immersion for more than 24 hours, corrosion processes were controlled by the diffusion of the corrosion products.

In the case of aluminum alloys, the PEO coatings are mainly composed of α-Al2O3 and γ-Al2O3 with some complex Al–Si–O phases also present. The relative phase amount, pore size, corrosion resistance and other properties of the coatings are significantly influenced by the PEO electrolyte concentration and compositions, and on the magnitude of the process parameters. Where the constituents of electrolyte participated in film formation reaction

during the PEO process, the structure, composition and other properties of PEO films would vary with the electrolyte compositions. The amount of the harder α-Al2O3 phase could be increased by raising the current density [60]. For PEO coatings, the type of electrolyte is selected according to the substrate involved and the desired properties of the coating [82]. Higher sodium silicate concentration in the electrolyte results in higher growth rates, which may attributed to: more silicate is co-deposited with substrate oxidation and that an increase of the concentrations depresses oxide dissolution and the layer growth rate is increased [30]. It has been reported that phosphate was useful in enhancing the corrosion resistance of inner barrier layer of PEO coatings on aluminum alloys [83]. When the sodium tungstate concentration increases, the coating becomes thicker, contains more α-Al2O3, and has higher micro hardness and corrosion resistance. Li et al [84] obtained hard corrosion resistant alumina coating on Al-Si alloy in borate electrolyte. A similar improvement was also achieved for other aluminum alloys, including Al-Cu, Al-Mg and Al-Zn-Mg [85].

Khan et al [86], and Hussein et al [87], studied the PEO coatings on aluminum formed by unipolar and bipolar pulsed current methods. A bipolar current mode provides better corrosion resistance than unipolar mode due to the reduction of the pores and coating defects. Xue et al [88] through elemental analysis across the cross section of the coating performed after corrosion tests detected the presence of chloride ions only in the porous layer and not in the compact inner layer. Hence the corrosion resistance of the PEO coating is mainly derived from the inner compact layer. The evolution of impedance spectra with time, in general shows good correlation between the morphology of the oxide coating and the corrosion performance over a period of time.

8.3. Ti-alloys

Titanium and Ti alloys are remarkably resistant to corrosion owing to the formation of stable, self-healing oxide films on their surfaces. The major corrosion problem with Ti alloys may be in acidic environments, particularly when the acid concentration and temperature increase. In this case, the oxide film on Ti deteriorates and dissolves and the unprotected metal is oxidized to the soluble trivalent ion [89]. The PEO process has been recently used to prepare a porous and adherent titania coating which enhances corrosion resistance [90–93], bioactivity [94,95], and greater biocompatibility. Because the performance of PEO coatings strongly depends on the experimental conditions, such as the properties of the electrolyte and the PEO operation power, there are many reports on the relationship between the coating performance and the operation conditions. Zhang et al [96] conclude from EIS studies that the addition of calcium hypophosphite has significant influence on the growth process during the PEO coating stages prepared on a Ti6Al4V alloy under DC power. The equivalent circuit shown in Fig. 18 was used to analyze the EIS results in their study, where Rs is the electrolyte resistance; Q1 and Q2 model the electrical properties of the outer and inner layers, respectively; Rpo is the resistance of the electrolyte saturating the outer layer; and R2 represents the resistance of the inner layer. Here, Q, a constant phase element (CPE), is used to replace the pure capacitance. The equivalent circuits employed for curve fitting of the uncoated sample is illustrated in Fig. 18(b) where R_{CT}

http://dx.doi.org/10.5772/57171

represent the charge-transfer resistance of the naturally formed oxide film on Ti. XRD analysis by Li et al [97] shows that the 110 μm ceramic coating prepared on TiAl alloy by PEO method consisted of three layers: dense layer composed of Al2TiO5 and TiO2 rutile phases, intermediate layer and loose layer contained a large amount of amorphous SiO2 besides Al2TiO5 and TiO2 rutile phases. The electrochemical corrosion experiments showed that the coatings produced using both unipolar and bipolar current modes successfully improved the corrosion resistance in comparison with the uncoated material [44]. The corrosion resistance of the PEO-coated specimens was mainly determined by the thickness, composition and quality of the dense inner layer. Hussein et al [44] studies for Ti6Al4V indicated that the PEO coating led not only to decrease of cathodic process, but also appearance of a large passivation plateau on the anodic polarization curves. As the inner layer of PEO coating is a barrier layer to decrease the corrosion rate of the substrate, it is expected that the protection efficiency strongly depended on the thickness and density of the inner layer coatings.

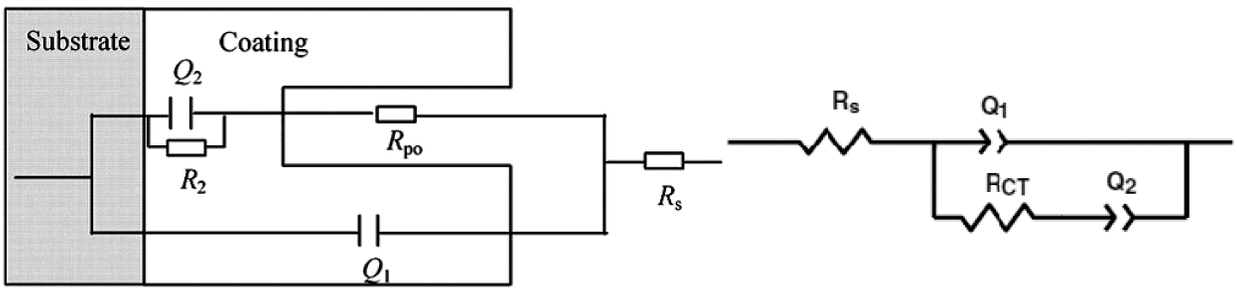

Figure 18. (a) Schematic of coatings and equivalent circuit used to model EIS results [96], (b) the equivalent circuit model for uncoated samples.

High applied voltage during PEO process can accelerate the migration process of the ions in electrolyte, which attracts the Ca2+ and PO43− ions to incorporate into the oxide layer by the electric field on the electrode and promotes the formation of the bioactive apatite [98]. On the other hand, the strong discharge phenomenon generated by high applied voltage increases the pore size which and decreases the density of the coating [99]. The longer immersion in simulated body fluid brings corrosive ions to penetrate through the porous layer resulting in the serious corrosion of the coated titanium alloy [100]. Moreover, cracks and poor adhesion easily arise from high applied voltage. Therefore, it is a key issue how to improve the corrosion resistance of the porous PEO coating with high bioactivity so as to alleviate toxicity and allergic reactions inside a living creature due to the release of metal ions to the adjacent tissue. By adjusting PEO parameters, including: current mode and density, treatment time and electrolyte composition and concentration, the distribution thickness between dense inner layer and porous outer layer and the structure of the coating can be controlled [92]. The compositional and morphological flexibility of coatings characteristic in PEO enables adjusting of calcium and phosphorus contents and structure of coatings favorable for bio adhesion between bone tissue and the implant [101].

9. Conclusions

This chapter has demonstrated that several coating systems can be used to provide improved corrosion protection of (Al, Mg, Ti) alloys. The current coating schemes are complex, multilayer systems that incorporate many different technologies and must be conducted very carefully in order to adequately protect light weight metals from corrosion in harsh service conditions. In order to achieve optimum adhesion, one of the most widely used coating methods for corrosion protection is through the PEO technique. A PEO process can be used to produce an oxide layer on light weight elements using different electrolyte and/or current modes which significantly affect coating morphology and microstructure and hence, corrosion resistance. A dense coating morphology could be achieved by adjusting positive to negative current ratio and their timing to eliminate or reduce the strongest plasma discharges. The rates of growth of the oxide outer and inner layers are processes parameter dependent. They result from a combination of three processes namely, (i) discharge processes causing the substrate to melt and oxidize when flowing out through the discharge channels and rapidly cooled at the surface–electrolyte interface, (ii) partial destruction of the outer layer due to strong discharges and (iii) diffusion processes.

Potentiodynamic polarization corrosion tests and EIS results both showed that PEO coatings significantly increased the corrosion resistance of light weight alloys and the degree of protection is affected by the amount of porosity and other coating defects which control the penetration rate of the electrolyte into the PEO coating. The scope for industrial use of this technology is quite promising due to the process flexibility, low capital cost and the environmentally-friendly precursor materials that are utilized. However, major uncertainties remain concerning process optimization, control and consistency (repeatability). Further improvement and developments are taking place in PEO technology, particularly to produce composite coatings by co-deposition of materials, including polymers and organic materials, within and/or at the top of the PEO layers.

10. Future trends

Research continues to be directed to identifying and developing new coating materials for automotive, aerospace, defense, textile, motor sports, electronics and oil and gas sectors. This is driven by the need for improved performance, reduced weight, increased multi-functionality and greater durability and also for reduced environmental hazards. Corrosion and wear resistance are traditional areas receiving the greatest attention. Both magnesium and aluminum alloys require an appropriate surface treatment to protect than against corrosion. PEO is certainly one of the most promising surface treatments for light weight alloys and is already in use for a number of applications, and as a replacement for hard anodizing especially for aluminum alloys. In addition to the excellent adhesion to the substrate, PEO coatings have higher thermal shock resistance, high dielectric strength and good optical properties. Using PEO coatings as a pre-treatment, followed by a second different coatings process (hybrid

coatings) to seal the unavoidable open pores and cracks formed during PEO coating, the corrosion resistance of PEO coatings can be further improved for long immersion times or corrosion in very aggressive environments. However, the porous structure of the PEO coating is necessary because they offer good adhesion if used as a pre-treatment for biocompatibility or decorative applications. While PEO has become increasingly popular in order to compete with other processes, further improvements are essential for optimizing the process and to reduce costs. The capital costs, electricity consumption and process control and reproducibility are critical aspects to be worked on.

Author details

Riyad O. Hussein and Derek O. Northwood

Department of Mechanical, Automotive and Materials Engineering, University of Windsor, Windsor, ON, Canada

References

[1] Park RM, Bena JF, Stayner LT, Smith RJ, Gibb HJ, Lees PSJ (2004). Hexavalent chromium and lung cancer in the chromate industry, a quantitative risk assessment. Risk Anal, 24(5),1099-1108.

[2] Walsh FC, Low CTJ, Wood RJK, Stevens KT, Archer J, Poeton AR, et al. Review. (2009) Plasma electrolytic oxidation (PEO) for production of anodised coatings on lightweight metal (Al, Mg, Ti) alloys. Transactions of the Institute of Metal Finishing 87(3), 122–35.

[3] Yerokhin AL. Nie X, Leyland A, Matthews A and Dowey S J (1999), Plasma electrolysis for surface engineering. Surf. Coat. Technol., 122(2-3), 73-93.

[4] Hussein RO, Nie X, Northwood DO, Yerokhin A, Matthews A (2010), Spectroscopic study of electrolytic plasma and discharging behaviour during the plasma electrolytic oxidation (PEO) process. Journal of Physics D: Applied Physics, 43, 105203.

[5] Hornberger H, Virtanen S, Boccaccini AR (2012), Biomedical coatings on magnesium alloys – A review, Acta Biomaterialia 8, 2442–2455.

[6] Pardo A, Casajús P, Mohedano M, Mohedano M, Coy A E, Viejo F, Torres B, Matykina E, (2009) Corrosion protection of Mg/Al alloys by thermal sprayed aluminium coatings. Applied Surface Science, 255, 6968-6977.

[7] Li JN, Cao P, Zhang XN, Zhang SX, He YH. (2010) In vitro degradation and cell attachment of a PLGA coated biodegradable Mg–6Zn based alloy. J Mater Sci, 45, 6038–45.

[8] Xu X, Lu P, Guo M, Fang M. (2010) Cross-linked gelatin/nanoparticles composite coating on micro-arc oxidation film for corrosion and drug release. Applied Surface Science, 256, 2367–71.

[9] Goueffon Y, Arurault L, Mabruc C, Tonond C, Guiguea P, (2009) Black anodic coatings for space applications, Study of the process parameters, characteristics and mechanical properties, Journal of Materials Processing Technology 209, 5145–5151.

[10] Shrestha S (2010) 'Magnesium and Surface Engineering-Technology Vision', Editorial in Surface Engineering, 26, (313-316).

[11] Gunterschulze A, Betz H, ElektrolytKondensatoren (Herbert Cram, Berlin, 1937; Oborongiz, Moscow, 1938) [in German and in Russian].

[12] Hussein RO, Nie X, Northwood DO (2013), The Application of Plasma Electrolytic Oxidation (PEO) to the Production of Corrosion Resistant Coatings on Magnesium Alloys, a Review. Corrosion and Materials, 38[1], 55-65.

[13] Walsh FC, Low CTJ, Wood RJK, Stevens KT, Archer J, Poeton AR and Ryder A, (2009) Plasma electrolytic oxidation (PEO) for production of anodised coatings on lightweight metal (Al, Mg, Ti) alloys, Transactions of the Institute of Metal Finishing, 87, 122-135.

[14] Sundararajan G and Rama L, (2003) Mechanisms underlying the formation of thick alumina coatings through the MAO coating technology. Surf. Coat. Technol., 167(2-3), 269-277.

[15] Duan H, Yan C, Wang F (2007) Effect of electrolyte additives on performance of plasma electrolytic oxidation films formed on magnesium alloy AZ91D Electrochimica Acta, 52, 3785-3793.

[16] Suminov IV, Apelfeld AV, Ludin VB, Krit BL and Borisov AM, (2005) Microarc oxidation theory, technology and equipment, Moscow Ecomet, ISBN 5-89594-110-9.

[17] Jaspard-Mécuson F, Czerwiec T, Henrion G, Belmonte T, Dujardin L, Viola A and Beauvir J, (2007) Tailored aluminium oxide layers by bipolar current adjustment in the Plasma Electrolytic Oxidation (PEO) process. Surf. Coat. Technol., 201(21), 8677-8682.

[18] Bala Srinivasan P, Liang J, Blawert C, Stormer M, Dietzel W, (2009) Effect of current density on the microstructure and corrosion behaviour of plasma electrolytic oxidation treated AM50 magnesium alloy, Applied Surface Science 255, 4212–4218.

[19] Hussein RO, Nie X, Northwood DO (2013), An investigation of ceramic coating growth mechanisms in Plasma Electrolytic Oxidation (PEO) processing, submitted to Electrochimica Acta, 112, 111-119

[20] Curran J A, Kalkanc H, Magurova Y and Clyne T W (2007), 'Mullite-rich plasma electrolytic oxide coatings for thermal barrier applications', Surf Coat Technol, 201, 8683–8687.

[21] Krishna L R, Purnima A S and Sundararajan G (2006), 'A comparative study of tribological behavior of microarc oxidation and hard-anodized coatings', Wear, 261, 1095–1101.

[22] Zhang P, Nie X, and Hu H, (2009) Wear and Galvanic Corrosion Protection of Mg alloy via Plasma Electrolytic Oxidation Process for Mg Engine Application, SAE Technical Paper 2009-01-0790, doi:10.4271/2009-01-0790.

[23] Frauchiger V M, Schlottig F, Gasser B and Textor M (2004), 'Anodic plasma–chemical treatment of CP titanium surfaces for biomedical applications', Biomaterials, 25, 593–606.

[24] Wang K, Kim Y, Hayashi Y, Lee C, Koo B, (2009) Ceramic coatings on 6061 Al alloys by plasma electrolytic oxidation under different AC voltages, J. Ceramic Processing Research. 10, 562-566

[25] Arrabal R, Matykina E, Hashimoto T, Skeldon P, Thompson GE (2009), Characterization of AC PEO coatings on magnesium alloys, Surf. Coat. Technol., 203, 2207-2220.

[26] Xu W, Jin Q, Zhua Q, Hu M and Ma Y, (2009) Anti-corrosion microarc oxidation coatings on SiCP/AZ31 magnesium matrix composite, Journal of Alloys and Compounds 482, 208-212.

[27] Curran JA, Clyne TW, (2005) Thermo-physical properties of plasma electrolytic oxide coatings on aluminium, Surf. Coat. Technol., 199, 168–176.

[28] Hussein RO, Zhang P, Xia Y, Nie X and Northwood DO (2011) The effect of current mode and discharge type on the corrosion resistance of plasma electrolytic oxidation (PEO) coated magnesium alloy AJ62, Surf. Coat. Technol., 206(7), 1990-1997

[29] Paul W, Sharma CP. (2006) Nanoceramic matrices, biomedical applications. Am J Biochem Biotechnol 2, 41–8.

[30] Yerokhin AL, Shatrov A, Samsonov V, Shashkov P, Pilkington A, Leyland A, Matthews A. (2005) "Oxide ceramic coatings on aluminium alloys produced by a pulsed bipolar plasma electrolytic oxidation process," Surf. Coat. Technol., 199, 150-157.

[31] Sundararajan G and Rama L, (2003) Mechanisms underlying the formation of thick alumina coatings through the MAO coating technology. Surf. Coat. Technol., 167(2-3), 269-277.

[32] Nie X, Meletis E I, Jiang J, Leyland A, Matthews A (2002) Abrasive wear/corrosion properties and TEM analysis of Al_2O_3 coatings fabricated using plasma electrolysis, Surf. Coat. Technol. 149, 245-251.

[33] Dunleavy CS, Golosnoy I O, Curran J A and Clyne T W, (2009) Characterisation of discharge events during plasma electrolytic oxidation. Surf. Coat. Technol., 203(22), 3410-3419.

[34] Ma Y, Nie X, Northwood DO and Hu H, (2004) Corrosion and erosion properties of silicate and phosphate coatings on magnesium. Thin Solid Films, 469-470, 472-477.

[35] Lee K, Lee B, Yoon S, Lee E, Yoo B, Shin D, (2012) Evaluation of plasma temperature during plasma oxidation processing of AZ91Mg alloy through analysis of the melting behavior of incorporated particles, Electrochimica Acta 67, 6-11

[36] Fournier V, Marcus P, Olefjord I, (2002), Oxidation of magnesium, Surface and Interface Analysis 34(1), 494-497.

[37] Nie X, Meletis E I, Leyland A, Matthews A, (2001), Effects of Solution pH and Electrical Parameters on Hydroxyapatite Coatings Deposited by a Plasma-assisted Electrophoresis Technique, J. of Biomedical Material Research 57, 612-618.

[38] Shi-Gang X, Li-Xin S, Rong-Gen Z, and Xing-Fang H, (2005) "Properties of aluminium oxide coating on aluminium alloy produced by micro-arc oxidation," Surf. Coat. Technol., 199, 184-188.

[39] Hussein RO, Nie X and Northwood DO (2010), Influence of process parameters on electrolytic plasma discharging behavior and aluminum oxide coating microstructure, Surf. Coat. Technol., 205, 1659-1667.

[40] Snizhko LO, Yerokhin AL, Pilkington A, Gurevina NL, Misnyankin DO, Leyland A, Matthews A. (2004) Anodic processes in plasma electrolytic oxidation of aluminium in alkaline solutions. Electrochimica Acta., 49[13], 2085-2095.

[41] Xue W, Deng Z, Chen R, Zhang T. (2000) Growth Regularity of Ceramic Coatings Formed by Microarc Oxidation on Al-Cu-Mg alloy. Thin Solid Films,372, 114-117.

[42] Chang L (2009) Growth regularity of ceramic coating on magnesium alloy by plasma electrolytic oxidation. Journal of Alloys and Compounds, 468, 462–465.

[43] Yerokhin AL, Leyland A, Matthews A (2002), Kinetic aspects of aluminium titanate layer formation on titanium alloys by plasma electrolytic oxidation, Applied. Surface. Science, 200, 172-184.

[44] Hussein RO, Nie X, Northwood DO, (2012) A spectroscopic and microstructural study of oxide coatings produced on a Ti-6Al-4V alloy by Plasma Electrolytic Oxidation, Materials Chemistry and Physics 134, 484– 492.

[45] Yerokhin AL, Snizhko LO, Gurevina NL, Leyland A, Pilkington A, Matthews A, (2003) Discharge characterization in plasma electrolytic oxidation of aluminium. J. Phys. D: Appl. Phys. 36, 2110.

[46] Albella J M, Montero I and Martinez-Duart J M, Parkhutik V, (1991) Dielectric breakdown processes in anodic Ta2O5 and related oxides, J. Materials Science, 26[13] 3422-3432

[47] Epelfeld A V, Lyudin V B, Dunkin O N and Nevskaya O S (2000) Bull. Russ. Acad. Sci. Phys. 64, 610

[48] Ikonopisov S, Girginov A and Machkova A (1977b), 'Theory of electrical breakdown during formation of barrier anodic films', Electrochem Acta, 22(10), 1077–1082.

[49] Hickling A and Ingram M D (1964), Contact glow-discharge electrolysis, Trans. Faraday Soc. 60 (496, part 4) 783-793.

[50] Hussein RO, Northwood DO, Nie X, (2010) Coating growth behavior during the plasma electrolytic oxidation process, J. Vacuum Science & Technology A Vacuum Surfaces and Films, 28(4), 766-773.

[51] Rakoch AG, Khokhlov VV, Bautin VA, Lebedeva NA, Magurova YV, Bardin IV, (2006) Model concepts on the mechanism of microarc oxidation of metal materials and the control over this process, Protection of Metals and Physical Chemistry of Surfaces, 42, 158-169.

[52] Krishna LR, Somaraju KRC, Sundararajan G. (2003) The tribological performance of ultra-hard ceramic composite coatings obtained through microarc oxidation. Surf. Coat. Technol. 163 –164, 484–490.

[53] Mécuson F, Czerwiec T, Belmonte T, Dujardin L, Viola A, Henrion G (2005) Diagnostics of an electrolytic microarc process for aluminum alloy oxidation. Surf. Coat. Technol., 200, 804-808.

[54] Song G L, Atrens A, (1999) Corrosion mechanisms of magnesium alloys, Advanced Engineering Materials, 1, 11-33.

[55] Shi Z, Liu M, Atrens A, (2010) Measurement of the corrosion rate of magnesium alloys using Tafel extrapolation, Corrosion Science 52, 579–588.

[56] Gu XN, Li N, Zhou WR, Zheng YF, Zhao X, Cai QZ, (2011) Corrosion resistance and surface biocompatibility of a microarc oxidation coating on a Mg–Ca alloy, Acta Biomaterialia 7, 1880–1889.

[57] Song G, Atrens A, (2003) Understanding magnesium corrosion mechanism: a framework for improved alloy performance, Advanced Engineering Materials 5, 837-858.

[58] Huang VM, Wua S-L, Orazema ME, Pébèreb N, Tribollet B, Vivier V, (2011) Local electrochemical impedance spectroscopy: A review and some recent developments Electrochimica Acta 56, 8048– 8057

[59] Gao JH, Shi XY, Yang B, Hou SS, Meng EC, Guan FX, (2011) Fabrication and characterization of bioactive composite coatings on Mg–Zn–Ca alloy by MAO/ sol-gel. Journal of Material Science: Journal of Materials Science: Materials in Medicine 22, 1681–1687.

[60] Zhang XP, Zhao ZP, Wu FM, Wang YL, Wu J. (2007) Corrosion and wear resistance of AZ91D magnesium alloy with and without microarc oxidation coating in Hank's solution. Journal of Material Science, 42, 8523–8528.

[61] Xu X, Lu P, Guo M, Fang M. (2010) Cross-linked gelatin/nanoparticles composite coating on micro-arc oxidation film for corrosion and drug release. Applied Surface Science 256, 2367–71.

[62] Hyun Sam Ryu, Seong-Jae Mun, Tae Seop Lim, Hong-Chan Kim, Kwang-Seon Shin, and Seong-Hyeon Hong, (2011) "Microstructure Evolution During Plasma Electrolytic Oxidation and Its Effects on the Electrochemical Properties of AZ91D Mg Alloy", Journal of The Electrochemical Society, 158 (9) C266-C273.

[63] Barik RC, Wharton JA, Wood RJK, Stokes KR, Jones RL, 167 (2005) Corrosion, erosion and erosion–corrosion performance of plasma electrolytic oxidation (PEO) deposited Al_2O_3 coatings, Surf. Coat. Technol., 199, 158-167.

[64] Gnedenkov AS, Sinebryukhov SL, Mashtalyar DV, Gnedenkov SV, (2013) Features of the corrosion processes development at the magnesium alloys surface, Surf. Coat. Technol., 225, 112–118.

[65] Williams G, Neil McMurray H, (2008), Localized corrosion of magnesium in chloride-containing electrolyte studied by a scanning vibrating electrode technique, J. Electrochemical Society, 155 (7), C340-C349.

[66] Ma Y, Nie X, Northwood DO and Hu H, (2006) Systematic study of the electrolytic plasma oxidation process on a Mg alloy for corrosion protection, Thin Solid Films 494, 296-301.

[67] Liang J, Hu L, Hao J, (2007) Characterization of microarc oxidation coatings formed on AM60B magnesium alloy in silicate and phosphate Electrolytes, Applied Surface Science, 253, 4490-4496.

[68] Liang J, Srinivasan PB, Blawert C, Dietzel W. (2010) Influence of chloride ion concentration on the electrochemical corrosion behavior of plasma electrolytic oxidation coated AM50 magnesium alloy, Electrochimica Acta, 55, 6802−6811.

[69] Ding J, Liang J, Li TH, Hao J, Xue Q (2007), Effects of sodium tungstate on characteristics of microarc oxidation coatings formed on magnesium alloy in silicate–KOH electrolyte,Transactions of Metals Society of China, 17, 244–249.

[70] Zhao F, Liao AD, Zhang RF, Zhang SF, Wang HX, Shi XM, Li MJ, He XM, (2010) Effects of sodium tungstate on properties of micro-arc coatings on magnesium alloys, Trans. Nonferrous Met. Soc. China, 20, s683- s687.

[71] Arabal R, Matykina E, Hashimoto T, Skeldon P and Thompson G E, (2009) Characterization of AC coatings in magnesium alloys, Surf. Coat. Technol., 203, 2207-2220.

[72] Barchiche C E, Rocca E, Juers C, Hazan J, Steinmetz J, (2007) Corrosion resistance of plasma anodized AZ91D magnesium alloy by electrochemical methods Electrochimica Acta 53, 417–425

[73] Duan H, Du K, Yan C, Wang F. (2006) Electrochemical corrosion behavior of composite coatings of sealed MAO film on magnesium alloy AZ91D, Electrochimica Acta 51, 2898–2908.

[74] Gu XN, Zheng W, Cheng Y, Zheng YF. (2009) A study on alkaline heat treated Mg–Ca alloy for the control of the biocorrosion rate. Acta Biomater, 5, 2790–2709.

[75] Chiu KY, Wong MH, Cheng FT, Man HC. (2007) Characterization and corrosion studies of fluoride conversion coating on degradable Mg implants. Surf. Coat. Technol., 202, 590–598.

[76] Song Y, Zhang S, Li J, Zhao C, Zhang X. (2010) Electrodeposition of Ca–P coatings on biodegradable Mg alloy: in vitro biomineralization behavior. Acta Biomater, 6, 1736–1742.

[77] Wong HM, Yeung KMK, Lam KO, Tam V, Chu PK, Luk KDK, (2010) A biodegradable polymer-based coating to control the performance of magnesium alloy orthopedic implants. Biomaterials,31, 2084–2096.

[78] Gu XN, Zheng YF, Lan QX, Cheng Y, Zhang ZX, Xi TF, Zhang DY, (2009) Surface modification of an Mg-1Ca alloy to slow down its biocorrosion by chitosan, Biomed Mater, 4, 044109.

[79] Arrabal R, Mota JM, Criado A, Pardo A, Mohedano M, Matykina E, (2012) Assessment of duplex coating combining plasma electrolytic oxidation and polymer layer on AZ31 magnesium alloy, Surf. Coat. Technol., 206,4692–4703.

[80] Wen L, Wang Y, Zhou Y, Ouyang J, Guo L, Jia D, (2010) Corrosion evaluation of microarc oxidation coatings formed on 2024 aluminium alloy, Corrosion Science 52, 2687–2696.

[81] Raj V, Ali M, (2009) Formation of ceramic alumina nanocomposite coatings on aluminium for enhanced corrosion resistance, J.Mats. Proc. Techn. 209, 5341–5352

[82] Lv G, Gu W, Chen H, Feng W, Khosa M, Li L, Nie L, Zhang F, Yang G, Si Z, (2006) Characteristics of ceramic coatings on aluminium by plasma electrolytic oxidation in silicate phosphates electrolytes. Appl. Surf. Sci. 253, 2947–2952.

[83] Kurze P, Schrekenbach J, Schwarz T, Krysmann W, (1986) Besehichten durch anodische oxidation unter fuhentludung, Metalloberflaeche, 40, 539-544

[84] LI Hx, Rudnev VS, Zheng XH, Yarovaya TP, Song RG. (2008) Characterization of Al_2O_3 ceramic coatings on 6063 aluminum alloy prepared in borate electrolytes by micro arc oxidation. Journal of Alloys and Compounds, 462, 99-102.

[85] Tillous K, Toll-Douchanoy T, Bauer-Grosse E, Hericher L, Geandier G. (2009) Microstructure and phase composition of micro arc oxidation surface layers formed on aluminium and its alloys 2214-T6 and 7050-T74. Surf. & Coat. Technol,, 203, 2969-2973.

[86] Khan HU, Yerokhin AL, Pilkington T, Leyland A, Mathews A, (2005) Residual stresses in plasma electrolytic oxidation coatings on aluminium alloys produced by pulsed unipolar current. Surf. Coat. Technol. 200, 1580–1586.

[87] Hussein RO, Nie X, Northwood DO, (2010) Influence of process parameters on electrolytic plasma discharging behaviour and aluminum oxide coating microstructure Surf. Coat. Technol., 205, 1659-1667

[88] Xue Wen-bin, Wang Chao, Tian Hua, Lai Yong-chun. (2007) Corrosion behaviours and galvanic studies of micro arc oxidation films on Al-Zn-Mg-Cu alloys, Surf & Coat Technol, 201, 8695-8701.

[89] Donachie MJ, (2000) Titanium: A Technical Guide, 2nd edition, ASM International, Materials Park, OH, p. 225.

[90] Wheeler JM, Collier CA, Paillard JM, Curran JA, (2010) Evaluation of micromechanical behaviour of plasma electrolytic oxidation (PEO) coatings on Ti-6Al-4V, Surf. Coat. Technol. 204, 3399-3409.

[91] Walsh FC, Low CTJ, Wood RJK, Stevens KT, Archer J, Poeton AR, Ryder A, (2009) Plasma electrolytic oxidation (PEO) for production of anodised coatings on lightweight metal (Al, Mg, Ti) alloys, Trans. Inst. Met. Finish. 87 (3), 122–135.

[92] Matykina E, Skeldon P, Thompson GE, (2009) Fundamental and practical evaluations of PEO coatings of titanium, Int. Heat Treat. Surf. Eng. 3 (1,2), 45-51.

[93] Yao Z, Liu Y, Xu Y, Jiang Z, Wang F, (2011) Effects of cathode pulse at high frequency on structure and composition of Al2TiO5 ceramic coatings on Ti alloy by plasma electrolytic oxidation, Mater. Chem. Phys. 126, 227–231.

[94] Frauchigera VM, Schlottigb F, Gasserc B, Textora M, (2004) Anodic plasma-chemical treatment of CP titanium surfaces for biomedical applications, Biomaterials 25, 593–606.

[95] Cui WF, Jin L, Zhou L, (2013) Surface characteristics and electrochemical corrosion behavior of a pre-anodized microarc oxidation coating on titanium alloy, Mater. Sci. Eng., C, 33, 3775-3779

[96] Zhang X L, Jiang Z H, Yao Z P, Wu Z D, (2010) Electrochemical study of growth behaviour of plasma electrolytic oxidation coating on Ti6Al4V: Effects of the additive, Corrosion Science, 52 3465-3473.

[97] Li X, Chenga G, Xuea W, Zheng R, Chengc Y, (2008) Wear and corrosion resistant coatings formed by microarc oxidation on TiAl alloy, Materials Chemistry and Physics 107, 148–152.

[98] Montazeri M, Dehghanian C, Shokouhfar M, Baradaran A, (2011) Investigation of the voltage and time effects on the formation of hydroxyapatite-containing titania prepared by plasma electrolytic oxidation on Ti-6Al-4V alloy and its corrosion behavior, Applied Surface Science, 257 7268-7275.

[99] Li L H, Kong Y M, Kim H W, (2004) Improved biological performance of Ti implants due to surface modification by micro-arc oxidation, Biomaterials 25, 2867-2875.

[100] Bai, YJ, Wang YB, Cheng Y, Deng F, Zheng YF, Wei SC, (2011) Comparative study on the corrosion behavior of Ti-Nb and TMA alloys for dental application in various artificial solutions. Mater. Sci. Eng. C Mater. Biol. Appl., 31, 702–711.

[101] Sul YT, Johansson CB, Petronis S, Krozer A, Jeong Y, Wennerberg A, Albrektsson T, (2002) Characteristics of the surface oxides on turned and electrochemically oxidized pure titanium implants up to dielectric breakdown: the oxide thickness, micropore configurations, surface roughness, crystal structure and chemical composition, Biomaterials, 23, 491– 501.

[102] Yao Z P, Wang D L, Xia Q X, Zhang Y J, Jiang Z H and Wang F P, (2012) Effect of PEO power modes on structure and corrosion resistance of ceramic coatings on AZ91D Mg alloy, Surface Engineering 28, 96-101.

[103] Zhou W, Shan D, Han E, Wei K, (2008) Structure and formation mechanism of phosphate conversion coating on die-cast AZ91D magnesium alloy, Corrosion Science 50, 329–337.

[104] Luo H, Cai Q, Wei B, Yu B, He J, Li D, (2009) Effect of (NaPO3)6 concentrations on corrosion resistance of plasma electrolytic oxidation coatings formed on AZ91D magnesium alloy, Journal of Alloys and Compounds, 474, 551-559.

[105] Luo H, Cai Q, Wei B, Yu B, Li D, He J, Liu Z, (2008) Effect of (NaPO3)6 concentrations on corrosion resistance of plasma electrolytic oxidation coatings formed on AZ91D magnesium alloy, Journal of Alloys and Compounds:464, 537–543.

[106] Yao Z, Li L, Jiang Z, (2009) Adjustment of the ratio of Ca/P in the ceramic coating on Mg alloy by plasma electrolytic oxidation, Applied Surface Science 255, 6724–8.

[107] Song YL, Liu YH, Yu SR, Zhu XY, Wang Q, (2008) Plasma electrolytic oxidation coating on AZ91 magnesium alloy modified by neodymium and its corrosion resistance, Applied Surface Science 254, 3014–3020.

IntechOpen